J. Astrophys. Astr. (2004) **25,** 1–55

Optical Variability Properties of High Luminosity AGN Classes

C. S. Stalin[1,2,3], Gopal-Krishna[2], Ram Sagar[1] & Paul J. Wiita[4]
[1]*Aryabhatta Research Institute of Observational Sciences (ARIES), Manora Peak Nainital 263 129, India.*
[2]*National Centre for Radio Astrophysics, TIFR, Pune University Campus, Pune 411 007, India.*
[3]*Laboratoire de Physique Corpusculaire et Cosmolgie, College de France, 11 pl. Marcelin Berthelot, F-75231, Paris Cedex 5, France.*
[4]*Department of Physics & Astronomy, MSC 8R0314, Georgia State University, Atlanta, Georgia 30303-3088, USA.*

Received 2003 June 24; accepted 2004 June 22

Abstract. We present the results of a comparative study of the intra-night optical variability (INOV) characteristics of radio-loud and radio-quiet quasars, which involves a systematic intra-night optical monitoring of seven sets of high luminosity AGNs covering the redshift range $z \simeq 0.2$ to $z \simeq 2.2$. The sample, matched in the optical luminosity – redshift ($M_B - z$) plane, consists of seven radio-quiet quasars (RQQs), eight radio lobe-dominated quasars (LDQs), five radio core-dominated quasars (CDQs) and six BL Lac objects (BLs). Systematic CCD observations, aided by a careful data analysis procedure, have allowed us to detect INOV with amplitudes as low as about 1%. Present observations cover a total of 113 nights (720 hours) with only a single quasar monitored as continuously as possible on a given night. Considering the cases of only unambiguous detections of INOV we have estimated duty cycles (DCs) of 17%, 12%, 20% and 61% for RQQs, LDQs, CDQs, and BLs, respectively. The much lower amplitude and DC of INOV shown by RQQs compared to BLs may be understood in terms of their having optical synchrotron jets which are modestly misdirected from us. From our fairly extensive dataset, no general trend of a correlation between the INOV amplitude and the apparent optical brightness of the quasar is noticed. This suggests that the physical mechanisms of INOV and long term optical variability (LTOV) do not have a one-to-one relationship and different factors are involved. Also, the absence of a clear negative correlation between the INOV and LTOV characteristics of blazars of our sample points toward an inconspicuous contribution of accretion disk fluctuations to the observed INOV. The INOV duty cycle of the AGNs observed in this program suggests that INOV is associated predominantly with the highly polarized optical emission components. We also report new VLA imaging of two RQQs ($1029+329$ & $1252+020$) in our sample which has yielded a 5 GHz detection in one of them ($1252+020$; $S_{5\,\mathrm{GHz}} \simeq 1$ mJy).

Key words. Galaxies: active—galaxies: jets—galaxies: photometry—quasars: general.

1. Introduction

The question of why only a small fraction of quasars are radio-loud has been debated for almost forty years. Various arguments have been put forward to explain this apparent radio-loud/radio-quiet dichotomy. Although the existence of the dichotomy has even been questioned (e.g., Goldschmidt *et al.* 1999; White *et al.* 2000), a recent careful analysis of the tricky selection effects indicates that it may be real (Ivezic *et al.* 2002). It has been argued recently that the radio emission correlates with the mass of the nuclear black hole (e.g., Dunlop *et al.* 2003 and references therein); however, this assertion has been questioned (Ho 2002; Woo & Urry 2002). McLure & Dunlop (2001) stress the possible importance of accretion rate and changes in accretion mode to this dichotomy.

On the theoretical side, two main approaches have been put forward to explain this dichotomy. In one scenario, the jets in RQQs are absent or inherently weak. Some possible mechanisms identify this differentiating factor with the spin of the black hole (Wilson & Colbert 1995; Blandford 2000), or magnetic configurations (Meier 2002). Wills (1996) suggested that all quasars launch jets but those aimed into a galactic disk are destroyed by interactions with the dense gas and thus appear radio-quiet. An extreme variant of this possibility is the hypothesis that the relativistic jets in RQQs are largely snuffed out before escaping the nuclear region itself due to heavy inverse Compton losses (Kundt 2002). As a consequence, jets on radio emitting physical scales are quenched, even though they might emit substantial amounts of non-thermal optical synchrotron emission on micro-arcsecond scales. Unfortunately, such μ arcsec scales are beyond the reach of any existing imaging telescopes and the only way to probe their conditions is through flux variability observations.

Although intra-night optical variability (INOV) or "microvariability" was convincingly established for blazars over a decade ago (e.g., Miller, Carini & Goodrich 1989; Carini, Noble & Miller 1998), the question of whether RQQs also show INOV has remained controversial (Gopal-Krishna *et al.* 1995, 2000; Jang & Miller 1995, 1997; Rabbette *et al.* 1998; de Diego *et al.* 1998; Romero *et al.* 1999; Carini *et al.* 1999). Likewise, the cause of INOV is still a much debated issue. However, for blazars (CDQs and BL Lacs) which are believed to be dominated by non-thermal Doppler boosted emission from jets (e.g., Blandford & Rees 1978), the occurrence of rapid intensity variations in both the radio and optical bands is believed to be due to shocks propagating down their relativistic jets (e.g., Marscher & Gear 1985). Intra-night variability in blazars may well arise from instabilities or turbulent fluctuations in the flow of such jets (e.g., Hughes, Aller & Aller 1992; Marscher, Gear & Travis 1992). Alternate models, which invoke accretion disk instabilities or perturbations (e.g., Mangalam & Wiita 1993; for a review see Wiita 1996) may also explain INOV, particularly in RQQs, where any contribution from the jets, if they are at all present, is weak.

While conclusive evidence for the presence of jets in RQQs is far from clear, deep VLA observations hint at the presence of weak jets even in RQQs (Kellermann *et al.* 1989; Miller, Rawlings & Saunders 1993; Kellermann *et al.* 1994; Papadopoulos *et al.* 1995; Kukula *et al.* 1998; Blundell & Beasley 1998; Blundell & Rawlings 2001). The existence of incipient nuclear jets in RQQs have also been inferred from radio spectral index measurements of optically selected quasar samples (Falcke, Patnaik & Sherwood 1996). If indeed optical synchrotron jets exist even in RQQs, then a fairly

robust signature of such un-imageable (because at the micro-arcsecond scale) jets can come from detection of INOV at the level exhibited by their radio loud counterparts, namely the LDQs. To persue these issues, a project to search for INOV in the four major classes of powerful AGNs was initiated in 1998 as a collaborative effort between the Aryabhatta Research Institute of Observational Sciences (ARIES), Nainital and the National Centre for Radio Astrophysics (NCRA), Pune. The present paper presents the detailed results of this project, part of which has been published elsewhere (Gopal-Krishna *et al.* 2003, hereafter GSSW03; Stalin *et al.* 2004, SGSW04; Sagar *et al.* 2004, SSGW04).

2. Selection of the sample

AGNs in general, have very different observational characteristics including a huge range in luminosity, redshift and power across the electromagnetic spectrum. Also, the co-moving number density of quasars detected at a given absolute magnitude is found to undergo a rapid evolution with redshift (Schmidt & Green 1983; Boyle *et al.* 2000; Wisotzki 2000). Therefore, sample selection is crucial for studying INOV of quasars. To avoid selection biases introduced by differences in luminosity and redshift, the objects were selected such that all objects in a given set have similar optical magnitudes, in addition to having very similar redshifts; they are thus well matched in the optical luminosity–redshift plane. Our sample, selected from the catalog of Véron-Cetty & Véron (1998), consists of seven sets of AGNs covering a total redshift range from $z = 0.17$ to $z = 2.2$. Each set was designed to consist of a radio-quiet quasar (RQQ), a radio lobe-dominated quasar (LDQ), a radio core-dominated quasar (CDQ) and/or a BL Lac object (BL). These seven sets cover seven narrow redshift intervals centered at $z = 0.21$, 0.26, 0.35, 0.43, 0.51, 0.95 and 1.92. However, it was not possible to find seven complete sets that satisfied our other observationally dictated criteria (sufficiently bright to allow dense temporal sampling and having several suitable nearby comparison stars), so our entire sample actually consists of 26, not 28, QSOs with the distribution of 7 RQQs, 8 LDQs, 5 CDQs and 6 BLs. The slight unevenness in number is because the two QSOs $1308 + 326$ and $1512 + 370$ were initially selected as CDQs, but better radio data classified $1512 + 370$ as an LDQ (see SGSW04), while the blazar $1308 + 326$ was found to be a BL Lac (see SSGW04). Due to the paucity of BL Lacs at low z, one object ($1215 + 303$) serves as a member of both Sets 1 and 2, and none was available in the highest redshift bin. The general properties of the objects monitored in this program are given in Table 1.

The magnitude range for the QSOs in our sample is $-30.0 < M_B < -24.3$ (assuming $H_0 = 50\,\mathrm{km\ s^{-1}\ Mpc^{-1}}$, $q_0 = 0$). This implies that we are dealing with luminous AGNs, which are legitimately classified as QSOs, and in all cases the underlying galaxy contamination to the luminosity of the AGN is $< 10\%$. Moreover, since the AGN of the four different types are similarly distributed in the $z - M_B$ plane, this selection criterion minimises selection biases such as K-corrections, evolutionary effects and any other differences linked to redshift and luminosity. Conservatively, we have included in our sample only those RQQs for which the K-corrected ratio of 5 GHz to 2500 Å flux densities is less than 1 i.e., $R^* < 1$ (see Table 1) even though the usual criterion used to call a QSO an RQQ is $R < 10 (R = f(5\,\mathrm{GHz})/f(B)$; Kellermann *et al.* 1989).

Table 1. General information on radio-quiet, lobe-dominated, core-dominated and BL Lac objects monitored in the present programme.

Set no.	Object	Other name	Type	RA(2000)	Dec(2000)	B (mag)	M_B (mag)	z	%Pol† (opt)	log $R^{*\ddagger}$
1.	0945+438	US 995	RQQ	09 48 59.4	+43 35 18	16.45	−24.3	0.226	—	< -0.07
	2349−014	PKS 2349−01	LDQ	23 51 56.1	−01 09 13	15.45	−24.7	0.174	0.91	2.47
	1309+355	PG 1309+355	CDQ	13 12 17.7	+35 15 23	15.60	−24.7	0.184	0.31*	1.36
	1215+303	B2 1215+30	BL	12 17 52.0	+30 07 01	16.07	−24.8	0.237	8.0	2.63
2.	0514−005	1E 0514−0030	RQQ	05 16 33.5	−00 27 14	16.26	−25.1	0.291	—	< 0.06
	1004+130	PG 1004+130	LDQ	10 07 26.2	+12 48 56	15.28	−25.6	0.240	0.78	2.29
	1128+315	B2 1128+31	CDQ	11 31 09.4	+31 14 07	16.00	−25.3	0.289	0.62	2.43
3.	1252+020	Q 1252+0200	RQQ	12 55 19.7	+01 44 13	15.48	−26.2	0.345	—	−0.28
	0134+329	3C 48.0	LDQ	01 37 41.3	+33 09 35	16.62	−25.2	0.367	1.41	3.93
	1512+370	B2 1512+37	LDQ	15 14 43.0	+36 50 50	16.25	−25.6	0.370	1.17	3.57
	0851+202	OJ 287	BL	08 54 48.8	+20 06 30	15.91	−25.5	0.306	12.50	3.32
4.	1101+319	TON 52	RQQ	11 04 07.0	+31 41 11	16.00	−26.2	0.440	—	< -0.41
	1103−006	PKS 1103−006	LDQ	11 06 31.8	−00 52 53	16.39	−25.7	0.426	0.37	2.80
	1216−010	PKS 1216−010	CDQ	12 18 35.0	−01 19 54	16.17	−25.9	0.415	6.90**	2.34
	0735+178	PKS 0735+17	BL	07 38 07.4	+17 42 19	16.76	−25.4	>0.424	14.10	3.55
5.	1029+329	CSO 50	RQQ	10 32 06.0	+32 40 21	16.00	−26.7	0.560	—	< -0.64
	0709+370	B2 0709+37	LDQ	07 13 09.4	+36 56 07	15.66	−26.8	0.487	—	2.08
	0955+326	3C 232	CDQ	09 58 20.9	+32 24 02	15.88	−26.7	0.530	0.53	2.74
	0219+428	3C 66A	BL	02 22 39.6	+43 02 08	15.71	−26.5	0.444	11.70	2.83
6.	0748+294	QJ 0751+2919	RQQ	07 51 12.3	+29 19 38	15.00	−29.0	0.910	—	−0.68
	0350−073	3C 94	LDQ	03 52 30.6	−07 11 02	16.93	−27.2	0.962	1.42	3.07
	1308+326	B2 1308+32	BL	13 10 28.7	+32 20 44	15.61	−28.6	0.997	10.20	2.71
	0235+164	AO 0235+164	BL	02 38 38.9	+16 37 00	16.46	−27.6	0.940	14.90	3.29
7.	1017+279	TON 34	RQQ	10 19 56.6	+27 44 02	16.06	−29.8	1.918	—	< -0.49
	0012+305	B2 0012+30	LDQ	00 15 35.9	+30 52 30	16.30	−29.1	1.619	—	1.76
	1225+317	B2 1225+31	CDQ	12 28 24.8	+31 28 38	16.15	−30.0	2.219	0.16	2.26

‡R* is the ratio of the 5 GHz to 2500 Å flux densities calculated following Stocke *et al.* (1992).

†Optical polarization are from Wills *et al.* (1992) except those marked with * (Berriman *et al.* 1990) and ** (Hutsemekers & Lamy 2001).

3. Radio observations and reductions

Since radio flux data were not available for two of our QSOs ($1252+020$ and $1029+329$), in order to ascertain their radio classification, we took VLA[1] snapshots at 5 GHz in the BnC configuration, in a dual intermediate frequency mode with a total on-source integration time of 10 minutes. The resulting images, made using the CLEAN algorithm within the AIPS software, are shown in Fig. 1 (rms noise $\sim 50\mu$Jy). While the QSO $1252+020$ was found be associated with an extended weak radio source of 1 ± 0.1 mJy, the other QSO, $1029+329$, has no radio counterpart down to a 3-sigma limit of 0.15 mJy. Therefore both are properly classified as RQQs, with $R = 0.52$ and $R < 0.23$, respectively.

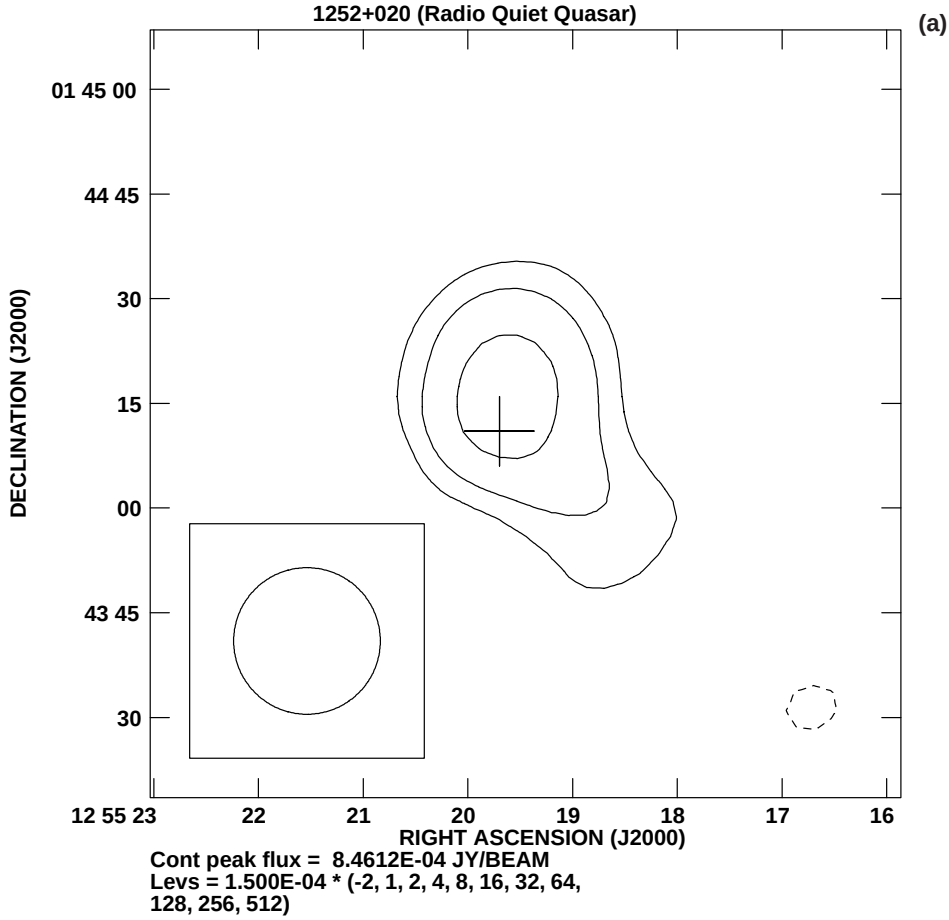

Figure 1. (*Continued*)

[1]The Very Large Array (VLA) of the National Radio Astronomy Observatory is operated by Associated Universities, Inc. under a cooperative agreement with the National Science Foundation.

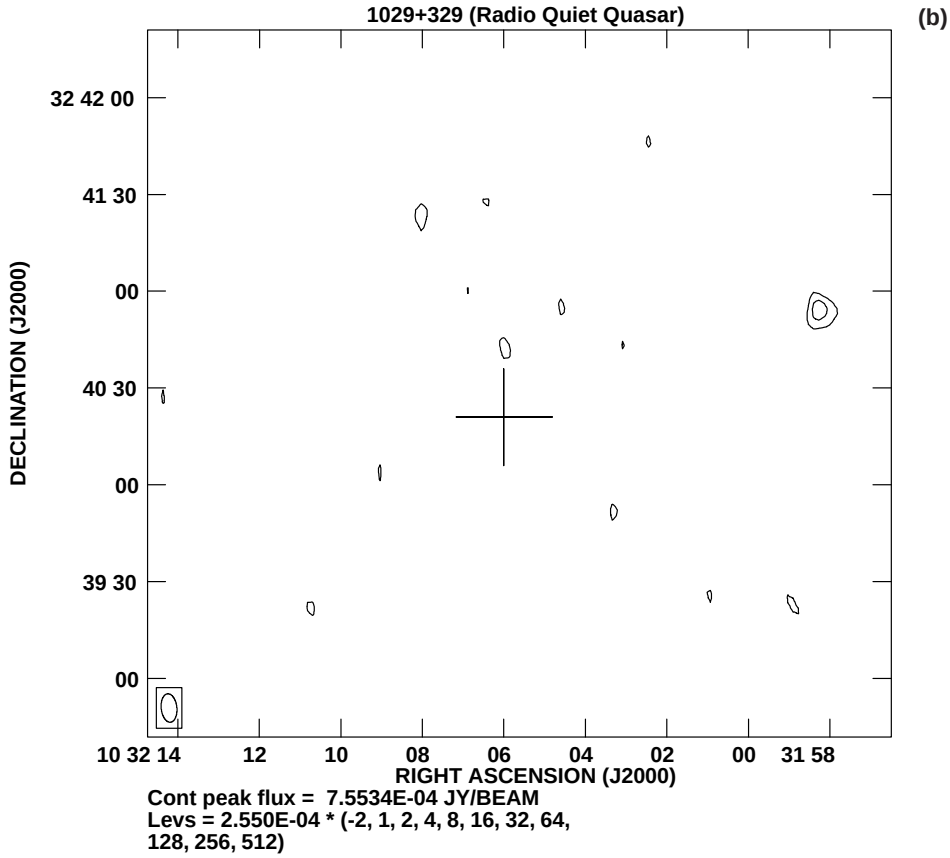

Figure 1(a–b). VLA 5 GHz total intensity images of the quasars 1252+020 (left) and 1029+329 (right). The synthesised beams are shown in the inset boxes.

4. Optical observations and data reductions

4.1 *The instrument*

The optical observations of the selected quasars were carried out using the 104 cm Sampurnanand telescope of the ARIES, Nainital. This is an RC system with a f/13 beam (Sagar 1999). The detector used for the observations was a cryogenically cooled $2048 \times 2048\,\mathrm{pixel}^2$ CCD, except prior to October 1999, when a smaller CCD of size $1024 \times 1024\,\mathrm{pixel}^2$ was used. In each CCD, a pixel corresponds to a square of 0.38 arcsec size, covering a total sky area of about $12' \times 12'$ in the case of larger CCD and about $6' \times 6'$ in the case of smaller CCD. To increase the S/N ratio, observations were carried out in 2×2 binned mode. Practically all the observations were carried out using R filter, except on two nights, where quasi-simultaneous R and I filter observations were done. The choice of the R filter in this observational program is because of its being at the maximum response of the CCD systems; thus the time resolution achievable for each object is maximised.

4.2 *Observing strategy*

The main goal of this program was to obtain lengthy temporally dense data trains for each object on each night it was observed, in order to be able to detect low level intra-night variations at high S/N. The optical monitoring of blazars has shown that the probability of observing INOV in a given night is greatly enhanced by continuous monitoring for at least 3 to 4 hours (Carini 1990). Accordingly, we attempted to monitor each object for a minimum of 5 hours per night, with a time resolution of the order of 10 minutes. However, on occasions when the object was in a faint state, the sampling time could be up to 30 minutes.

Another important strategy was to center the field of view so as to cover as many suitable comparison stars as possible within the CCD frame. For each of our quasars we could get at least two, but often more, comparison stars within 1 magnitude of the quasar's brightness in the frame. Several putative sources were eliminated from our sample if they had no suitable comparison stars in their vicinities. The availability of multiple comparison stars allowed us to identify and discount any comparison star which itself varied during a given night, thus allowing reliable differential photometry of the QSO. The positions and apparent B and R magnitudes of all the comparison stars used in our differential photometry are given in SGSW04 and SSGW04 and so will not be repeated here. The entire programme consists of observations on 113 nights from October 1998 through May 2002, adding up to 720 hours of useful observations (i.e., 6.4 hours/night on average). A log of the observations along with the basic results are given in Table 2.

4.3 *Data reduction*

Preliminary processing of the images as well as the photometry was done using the IRAF[2] software. The bias level of the CCD is determined from several bias frames (generally more than seven) taken intermittently during our observations over the night. A mean bias frame was formed using the task *zerocombine* in IRAF which was then subtracted from all the image frames of the night. Care was also taken in forming the mean bias frame such that they are not affected by cosmic-ray (CR) hits. The routine step of dark frame subtraction was not performed as the CCDs used in the observations were cryogenically cooled to -120° C at which temperature the amount of thermal charge is negligible for the exposure times of the present observations. Flat fielding was done by taking several twilight sky frames which were then median combined to generate the flat field template which was then used to derive the final frames; any errors in the flat field template were well within 0.1%. Finally CR hits seen in the flat fielded target frames were removed using the facilities available in MIDAS[3].

[2]IRAF is distributed by the National Optical Astronomy Observatories, which is operated by the Association of Universities for Research in Astronomy, Inc. under co-operative agreement with the National Science Foundation.

[3]MIDAS stands for Munich Image and Data Analysis System and has been designed and developed by the European Southern Observatory (ESO) in Munich, Germany.

Table 2. A log of observations and basic results of INOV of the QSOs.

Set no.	Object (type)	Date	N (obs)	T (hr)	INOV status*	$C_{\rm eff}^{\dagger}$	$\psi^{\dagger}$ %	$\tau^{\ddagger}$ (hr)	$P^{\ddagger}$ (hr)	$\eta_{\rm obs}^{\S}$	$\delta_{\rm obs}^{\S}$	Ref. to DLCs
1.	0945+438	15.01.99	44	8.0	NV							Present work
	(RQQ)	26.02.00	31	6.3	NV							Present work
		23.01.01	24	6.6	NV							Present work
	2349−01	13.10.01	34	6.8	V	3.6	2.2			0.02		SGSW04
	(LDQ)	17.10.01	39	7.6	V	3.1	1.5			0.02		SGSW04
		18.10.01	40	7.7	V	3.2	1.6	5.0		0.02		SGSW04
	1309+355	25.03.99	39	6.7	NV							Present work
	(CDQ)	01.04.01	32	4.6	NV							Present work
		02.04.01	41	5.2	NV							Present work
	1215+303	20.03.99	21	7.0	V	5.5	3.5	4.2		0.74	1.8	SSGW04
	(BL)	25.02.00	28	5.9	NV							Present work
		31.03.00	27	5.0	NV							Present work
		19.04.02	23	6.8	V	4.9	1.8	>6.8		0.05	1.0	SSGW04
2.	0514−005	09.12.01	25	5.3	NV							Present work
	(RQQ)	10.12.01	23	5.8	NV							Present work
		19.12.01	35	7.5	NV							Present work
	1004+130	27.02.99	30	4.3	NV							Present work
	(LDQ)	16.02.99	36	6.5	NV							Present work
		29.03.00	21	3.8	NV							Present work
		30.03.00	26	4.6	NV							Present work
		18.02.01	42	5.5	NV							Present work
		24.03.01	50	6.4	NV							SGSW04
	1128+315	18.01.01	31	5.7	NV							Present work
	(CDQ)	09.03.02	27	8.2	NV							SGSW04
		10.03.02	28	8.3	NV							Present work
3.	1252+020	22.03.99	36	6.4	V	3.3	2.3					SGSW04
	(RQQ)	09.03.00	29	6.1	NV							Present work
		03.04.00	19	4.3	V	3.6	0.9	>4.3		0.04		SGSW04
		26.04.01	20	4.6	NV							Present work
		18.03.02	19	7.3	NV							Present work

Table 2. (*Continued*)

Set no.	Object (type)	Date	N (obs)	T (hr)	INOV status*	$C_{\rm eff}^{\dagger}$	$\psi^{\dagger}$ %	$\tau^{\ddagger}$ (hr)	$P^{\ddagger}$ (hr)	$\eta_{\rm obs}^{\S}$	$\delta_{\rm obs}^{\S}$	Ref. to DLCs
3.	0134+329	07.11.01	33	6.5	NV							Present work
	(LDQ)	08.11.01	32	6.7	NV							Present work
		13.11.01	46	8.6	NV							Present work
	1512+370	23.03.02	24	7.0	NV							Present work
	(LDQ)	27.03.02	28	7.0	NV							Present work
		21.04.02	11	4.3	V	2.8	2.6	0.4		0.53	1.60	Present work
		23.04.02	15	5.3	NV							Present work
		01.05.02	19	6.6	V	3.0	3.9	0.4	1.8,3.4,5.6	0.18	1.29	Present work
	0851+202	29.12.98	19	6.8	V	2.8	2.3	>6.8		0.12	1.20	SSGW04
	(BL)	31.12.99	29	5.6	V	6.5	3.8	3.0		0.07	1.07	SSGW04
		28.03.00	22	4.2	V	5.8	5.0	1.2		0.88	1.77	SSGW04
		17.02.01	48	6.9	V	2.7	2.8	2.0	3.8	0.36	1.48	SSGW04
4.	1101+319	12.03.99	39	8.5	NV							Present work
	(RQQ)	04.04.00	22	5.6	NV							Present work
		21.04.01	21	6.1	V	2.6	1.2	0.8		0.11	1.17	SGSW04
		22.04.01	21	5.8	NV							Present work
	1103−006	17.03.99	23	3.8	NV							Present work
	(LDQ)	18.03.99	40	7.5	V	3.1	2.4	0.6		0.55	1.62	SGSW04
		06.04.00	13	3.9	PV	2.1	1.2					SGSW04
		25.03.01	28	7.2	NV							SGSW04
		14.04.01	19	4.5	NV							Present work
		22.03.02	15	5.8	PV	2.2	0.7					SGSW04
	1216−010	11.03.02	22	8.0	V	3.2	7.3	1.8	3.2	0.29	1.42	SSGW04
	(CDQ)	13.03.02	24	8.5	V	2.6	3.8	1.2	2.2	0.16	1.26	SSGW04
		15.03.02	11	3.9	V	3.9	5.5	1.0	2.2	0.77	1.73	SSGW04
		16.03.02	22	8.2	V	6.6	14.1	>8.2				SSGW04
	0735+178	26.12.98	49	7.8	NV							SGSW04
	(BL)	30.12.99	65	7.4	NV							Present work
		25.12.00	43	6.0	NV							Present work
		24.12.01	43	7.3	V	2.8	1.0	>8.1		0.05	1.00	SSGW04

Table 2. (*Continued*)

Set no.	Object (type)	Date	N (obs)	T (hr)	INOV status*	$C_{\rm eff}^{\dagger}$	$\psi^{\dagger}$ %	$\tau^{\ddagger}$ (hr)	$P^{\ddagger}$ (hr)	$\eta_{\rm obs}^{\S}$	$\delta_{\rm obs}^{\S}$	Ref. to DLCs
5.	1029+329	13.03.99	45	8.4	—	—	—	—	—	—	—	—
	(RQQ)	02.03.00	19	5.0	NV							Present work
		05.04.00	19	5.3	V	4.3	1.3	>6.2		0.13	1.21	SGSW04
		23.03.01	20	5.8	NV							Present work
		06.03.02	31	8.5	NV							SGSW04
		08.03.02	17	6.1	V	2.8	1.1					SGSW04
	0709+370	20.01.01	29	6.5	NV							Present work
	(LDQ)	21.01.01	29	6.2	NV							Present work
		25.01.01	31	7.1	NV							Present work
		20.12.01	49	7.9	V	3.1	1.4	4.4	7.0	0.007		SGSW04
		21.12.01	48	7.5	NV							Present work
	0955+326	19.02.99	36	6.5	NV							Present work
	(CDQ)	03.03.00	37	6.3	NV							Present work
		05.03.00	34	6.9	PV	2.2	0.7					SSGW04
	0219+428	14.11.98	118	6.5	V	6.0	5.4	>6.5		1.04	1.83	SSGW04
	(BL)	13.11.99	123	5.7	V	>6.6	5.5	>5.9		4.91	2.50	SSGW04
		24.10.00	73	9.1	V	5.8	4.3	>9.1		1.39	1.94	SSGW04
		26.10.00	82	10.1	V	3.5	3.2	4.9		1.14	1.87	SSGW04
		01.11.00	103	9.0	V	2.9	2.2	3.9		0.26	1.39	SSGW04
		24.11.00	71	5.1	NV							Present work
		01.12.00	59	5.1	V	>6.6	8.0	>5.1		2.14	2.12	SSGW04
6.	0748+294	14.12.98	22	7.6	NV							Present work
	(RQQ)	13.01.99	56	8.3	NV							Present work
		09.12.99	26	5.1	NV							Present work
		24.11.00	28	5.4	NV							Present work
		01.12.00	32	6.0	NV							SGSW04
		25.12.01	30	5.4	NV							SGSW04
	0350−073	14.11.01	31	6.6	NV							Present work
	(LDQ)	15.11.01	26	5.5	NV							Present work
		18.11.01	25	5.7	NV							Present work

Table 2. (*Continued*)

Set no.	Object (type)	Date	N (obs)	T (hr)	INOV status*	$C_{\rm eff}^{\dagger}$	$\psi^{\dagger}$ %	$\tau^{\ddagger}$ (hr)	$P^{\ddagger}$ (hr)	$\eta_{\rm obs}^{\S}$	$\delta_{\rm obs}^{\S}$	Ref. to DLCs
6.	1308+326	23.03.99	17	6.0	—	—	—	—	—	—	—	—
	(BL)	26.04.00	16	5.6	NV							Present work
		03.05.00	19	6.7	—	—	—	—	—	—	—	—
		17.03.02	19	7.7	V	3.1	3.4	1.2,4.4		5.39	2.55	SSGW04
		20.04.02	14	5.8	NV							Present work
		02.05.02	15	5.1	NV							Present work
	0235+164	13.11.98	36	4.4	—	—	—	—	—	—	—	—
	(BL)	12.11.99	39	6.6	V	>6.6	12.8	3.6		2.48	2.18	SSGW04
		14.11.99	34	6.2	V	3.2	10.3	3.4		1.23	1.90	SSGW04
		22.10.00	39	7.9	V	2.6	7.6			1.71	2.03	SSGW04
		28.10.00	29	6.8	—	—	—	—	—	—	—	—
7.	1017+279	14.03.99	43	7.3	NV							Present work
	(RQQ)	14.01.00	33	7.1	NV							Present work
		27.02.00	33	8.1	NV							Present work
	0012+305	18.01.01	17	3.6	NV							Present work
	(LDQ)	20.01.01	14	3.2	NV							Present work
		24.01.01	14	2.9	NV							Present work
		14.10.01	20	5.7	NV							Present work
		21.10.01	22	5.7	NV							SGSW04
		22.10.01	24	6.2	NV							Present work
	1225+317	07.03.99	49	6.6	NV							Present work
	(CDQ)	07.04.00	23	6.0	NV							Present work
		20.04.01	34	7.4	NV							Present work

*V (for variables); PV (for probable variables); NV (for non-variables); — (for poor data).
$^{\dagger}C_{\rm eff}$ and ψ indicate the statistical significance and amplitude of variability.
‡Variability timescales, τ, and "periods", P from structure functions.
§Efficiency, $\eta_{\rm obs}$, and Doppler factor, $\delta_{\rm obs}$, in the framework of relativistic beaming models.

4.4 *Photometry*

Aperture photometry on both the AGN and the comparison stars present on the flat-fielded CCD frames were carried out using the task *phot* in IRAF. A critical input to be specified to *phot* was the radius of the aperture used to perform the photometry. The selection of this aperture determines the S/N for each object in the frame. In an investigation by Howell (1989) the issue of an optimum aperture to maximize the S/N was discussed; this nominally optimum aperture is found to lie close to the FWHM of the PSF of the stars on the frame. By choosing an aperture that is relatively close to the FWHM of a source, clearly some of the total flux from the source will be left out of the aperture. However, in this work only magnitude differences, and not the absolute fluxes, are important. Hence, this procedure of selecting an optimum aperture was promising for enhancing the photometric precision of the observations, since the S/N was maximised. The procedure we followed for finding an optimum aperture was identical to that used in Noble (1995). We specified several aperture radii (starting from the median FWHM of the night and then incrementing by 0.2 pixels) and then identified the aperture that yielded magnitudes of stars such that the scatter or variance of the resulting steadiest pair of Star – Star differential light curves (DLCs) was minimised. This process of finding the optimum aperture is illustrated in Fig. 2, which shows five DLCs for the same pair of comparison stars in the field of the quasar $1017 + 279$ observed on 27th February 2000. The larger variance at small apertures is due to the inclusion of fewer source pixels, whereas the larger variance at large apertures is due to too many noise pixels compared to source pixels.

The local sky background (instead of a mean over the entire CCD chip) estimated around the QSO and each of the comparison stars is subtracted from the counts over the optimum aperture to get the instrumental magnitudes for generating the DLCs. This sky subtraction (with fluctuations across the CCD chip within 0.1%) is not a major issue in this technique of differential photometry. The overall errors due to flat fielding, background subtraction and any effects in the instrument during our observations are well below 0.3%, which is also the typical standard deviation attained in the DLCs involving comparison stars.

5. Potential sources of spurious intensity variations

5.1 *Variable seeing*

One potential source of spurious variability in aperture photometry is the contamination arising from the host galaxy of the AGN recorded on the CCD frame. This is because the surface brightness profile of any underlying galaxy will not respond to atmospheric seeing fluctuations in a manner similar to the central AGN. Thus, intra-night fluctuations in the seeing could result in the variable contribution from the host galaxy within the aperture, producing spurious changes in the brightness that could be mistaken for AGN variability. Recently the effect of spurious variations introduced in the DLCs by atmospheric seeing fluctuations has been quantitatively addressed by Cellone, Romero & Combi (2000) through extensive simulations. These authors conclude that spurious differential magnitude variations due to seeing fluctuation can be substantial for AGN with relatively brighter hosts (such as Seyfert galaxies) when too small photometric apertures are used.

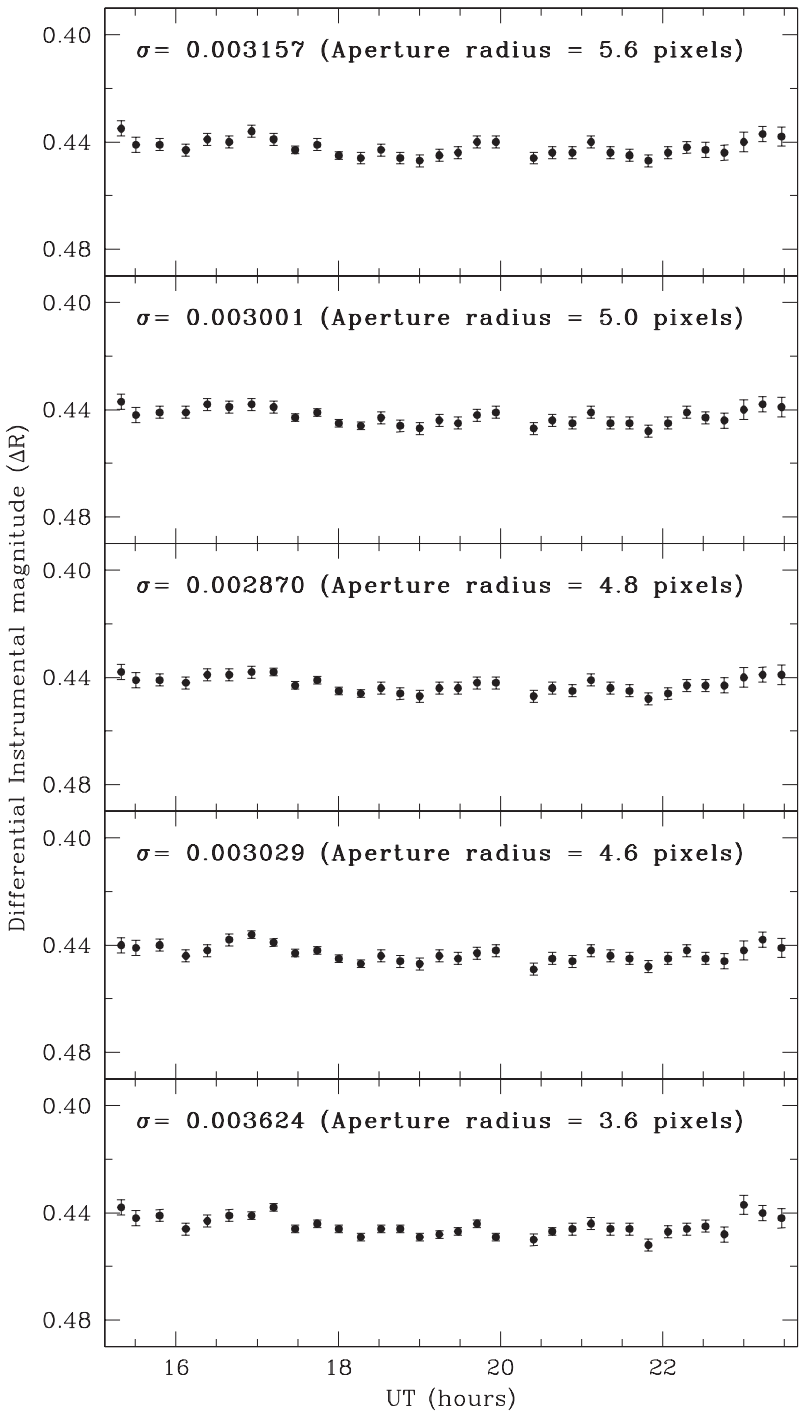

Figure 2. DLCs involving stars S2 and S3 in the field of the RQQ 1017 + 279 observed on 27th February 2000, for five different aperture radii showing the selection of optimum aperture. The minimum scatter occurs at an aperture radius of 4.8 pixels.

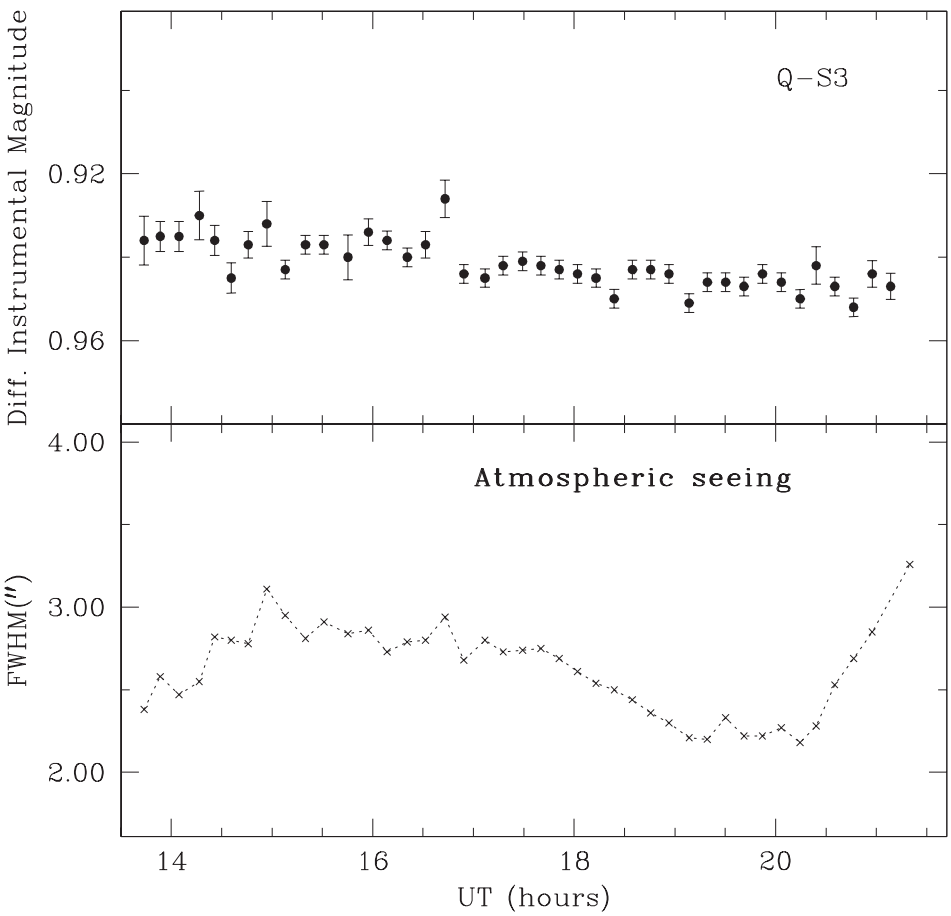

Figure 3. DLC of the LDQ 2349 − 014 observed on 17th October 2001 (top) and the variation of seeing during that night (bottom panel). The aperture radius used for the photometry is 5″.

Our data are very unlikely to be affected by this problem in any measurable sense, since all the AGNs in our sample are luminous ($M_B < -24.3$ mag); even though the host galaxies of powerful quasars are also typically fairly luminous galaxies, the nucleus is usually highly dominant *vis-à-vis* the host galaxy. In fact, the underlying host galaxy is not seen in any CCD images of our quasars except one, (LDQ 2349 − 014) which belongs to the lowest-redshift bin of our sample. We therefore conclude that except in the case of LDQ 2349 − 014, the host galaxies are fainter than $R \sim 19$ mag, while the quasars are brighter than $R \sim 17$ mag. Hence, applying the results of Cellone *et al.* (2000) for our quasar and host galaxy magnitudes and our adopted photometric apertures ranging from 3 to 7 arcsec, which are always rather large compared to the seeing FWHM lying between 1.4 and 4.4 arcsec, leads us to conclude that any such putative spurious variations should be well under 0.01 mag.

To explicitly consider the worst case scenario, Fig. 3 shows the DLC (with respect to Star 3) of the dimmest quasar relative to its host in our sample, LDQ 2349 − 014; also in this figure is the variation of atmospheric seeing during the observing night. If seeing variations were to play a role, one would expect to see the quasar plus host

galaxy appear to relatively brighten (dim) when the seeing is better (worse), as more (less) of the galaxy's light will be included in the aperture. As Fig. 3 shows, while the seeing worsened over the first hour or so of the observations the quasar remained essentially constant in luminosity; as the seeing improved between 17 and 20 UT the quasar dimmed slightly; and as the seeing dramatically worsened over the last hour of observations, the data became a little noisier but the mean quasar brightness didn't change. Either no (or a negative to the expected) correlation is found between the seeing variations and the DLC, thereby eliminating the possibility that the steady, slow decline seen in the quasar DLC is an artefact arising from the rather substantial seeing fluctuations.

5.2 *Effects of colours of the comparison stars*

Even on the clearest nights, objects are dimmed due to extinction by the Earth's atmosphere. The amount of dimming depends on the airmass, the wavelength of observation and the prevailing atmospheric conditions. The observed magnitude (m_λ) is related to the magnitude above the Earth atmosphere (m_{λ_o}) as (Henden & Kaitchuck 1982)

$$m_\lambda = m_{\lambda_o} + (K'_\lambda + K''_\lambda c)X, \tag{1}$$

where K'_λ and K''_λ are respectively the principal and second-order extinction coefficients, c is the colour index of the observed object and X is the airmass in the direction of the object. An advantage of performing differential photometry between the target and comparison stars located on the same CCD frame is that first-order extinction effects on the differential magnitude cancels out, as both the comparison stars and the target are seen through nearly identical atmospheric layers making the same X. However, K''_λ, which is applied to the colour of the object, can affect the differential magnitude. From equation (1) the differential magnitude between two objects of colour indices $c1$ and $c2$ is given by

$$\Delta m_\lambda = \Delta m_{\lambda_o} + K''_\lambda X \Delta c, \tag{2}$$

where $\Delta c = c1 - c2$, is the difference between the observed colour indices of the two objects. The relation between the standard and observed colour differences between the two objects can be written as

$$\Delta C = \mu \Delta c, \tag{3}$$

where $\Delta C = C1 - C2$, is the difference between the standard colour indices of the two objects. As μ is close to unity for the CCD systems used in the present observations, the observed colour index difference is not too different from the standard colour index difference. The values of $\Delta(B - R)$ between any quasar and comparison stars in our sample range between 0.4 and -2.5 mag. In order to investigate the effects of these colour differences on the DLCs of the quasars under study, the following analyses have been carried out.

From linear least square fitting of equation (2) for Δm_λ against Δc for the comparison stars using the standard colour index $C \equiv (B - R)$ taken from the United States Naval Observatory (USNO) catalog[4] to the observations we found that the effect of

[4]http://archive.eso.org/skycat/servers/usnoa.

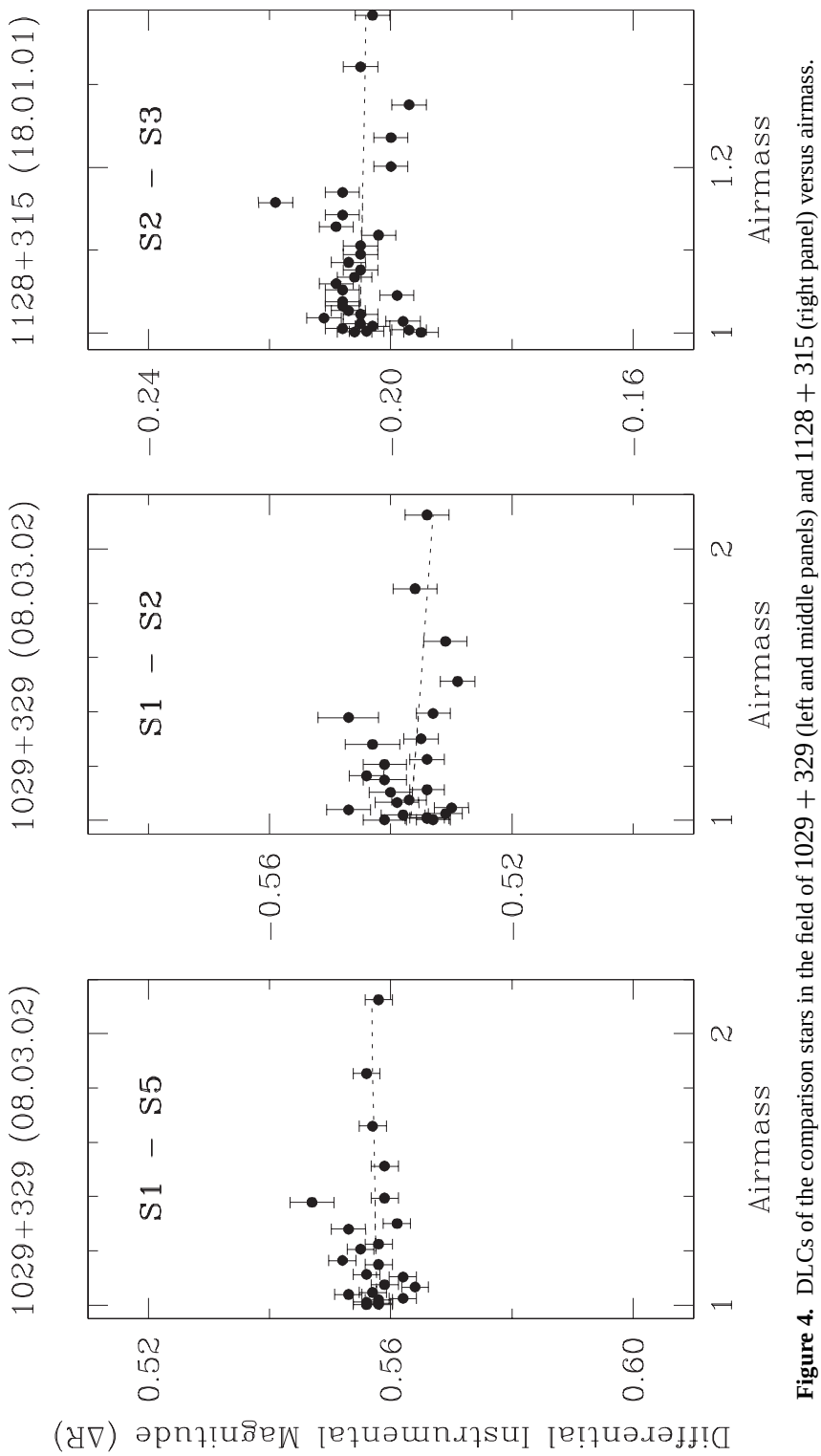

Figure 4. DLCs of the comparison stars in the field of 1029 + 329 (left and middle panels) and 1128 + 315 (right panel) versus airmass.

second-order extinction is virtually negligible, although we note that USNO magnitudes have errors of up to 0.3 mag. Therefore, to further carefully investigate the effect of colour differences between the objects on their observed DLCs, we have shown in Fig. 4 (left panel) the observed instrumental magnitude difference (Δm_λ in equation 2) between the stars S1 and S5 plotted against the airmass, whereas the middle panel shows the magnitude difference between S1 and S2 plotted against the airmass. Both of these DLCs are for the observations of the source $1029 + 329$ carried out on the night of 8th March 2002 up to a maximum hour angle of 5 hours corresponding to $X \simeq 2.2$. Observations on the other objects in our sample were rarely carried out at airmasses greater than this value. The colour difference $\Delta(\mathrm{B} - \mathrm{R})$ between S1 and S2 is 1.9 while between S1 and S5 it is 0.9. From Fig. 4 (left and middle panels) it is seen that despite a rather large range in airmass and a fairly large colour difference between the three stars, no artificial variations are introduced. Least square fits to the data sets shown in the left and middle panels of Fig. 4 yield slopes ($K''_\lambda \Delta c$ in equation 2) of -0.0008 ± 0.0023 and 0.0033 ± 0.0037, which are essentially zero. Also shown in Fig. 4 (right panel) is the observed instrumental magnitude difference between stars S2 and S3, having a large difference in colour index of -1.4, in the field of the QSO $1128 + 315$, as observed on 18th January 2001. Linear regression analysis yields a slope of 0.0026 ± 0.0089, which is again indistinguishable from zero. Any such effect is thus less than the photometric error of individual data points on the DLCs, and so we conclude that the colour differences between our sets of quasars and the comparison stars used in the differential photometry will not have any significant effects on the DLCs (see also GSSW03) even if account is taken of the errors in the magnitudes of the USNO catalog used for knowing the colours of the QSOs and stars. Similar conclusions were also drawn by Carini *et al.* (1992) in their study of rapid variability of blazars.

5.3 *Error estimation of the data points in the DLCs*

Determination of the basic variability parameters, such as peak-to-peak variability amplitudes, requires a realistic estimate of the photometric errors of individual data points of a given DLC. It has been argued recently in the literature that the photometric errors given by the reduction routines in IRAF and DAOPHOT underestimate the true errors. Considering the differences between the magnitudes of the added and recovered stars using the *addstar* routine of DAOPHOT, Gopal-Krishna *et al.* (1995) found that the formal errors returned by DAOPHOT are too small by a factor of about 1.75. Similarly, Garcia *et al.* (1999) found that the error given by the *phot* task in IRAF is underestimated by a median factor of 1.73. In this work we have made an independent estimate of this systematic error factor. To do this we have considered those 108 nights of observations (out of the total 113 nights) which we have found useful for INOV studies. Out of these, we have identified 74 DLCs pertaining to 'well behaved' (i.e., stable) comparison stars. Only the best available star—star DLC for each of these nights were considered. The unweighted mean of a DLC consisting of N data points having amplitude X_i, is given by

$$\langle X \rangle = \frac{1}{N} \sum_{i=1}^{N} X_i, \tag{4}$$

and the variance of the DLC is

$$S^2 = \frac{1}{N-1}\sum_{i=1}^{N}(X_i - \langle X\rangle)^2. \quad (5)$$

Both intrinsic source variability and measurement uncertainty contribute to this observed variance. Under the assumptions that both components are normally distributed and combine in quadrature the observed variance can be written as (see Edelson *et al.* 2002)

$$S^2 = \langle X\rangle^2\sigma_{XS}^2 + \langle\sigma_{err}^2\rangle. \quad (6)$$

The first term on the right represents the intrinsic scatter induced by source variability, and the second term is the contribution of measurement noise as returned by the *phot* task in IRAF. Assuming that the scatter of the data points is predominantly due to statistical uncertainty in the measurements, we have

$$\langle\sigma_{err}^2\rangle = \frac{1}{N}\sum_{i=1}^{N}\sigma_{err,i}^2. \quad (7)$$

As we have considered here only star–star DLCs, the contribution of source variability to the observed variance S^2 may be taken to be zero and therefore S^2 becomes equal to the average of the squares of the measurement errors $\langle\sigma_{err}^2\rangle$.

For each DLC we computed the quantity

$$Q = S^2 - \eta^2\langle\sigma_{err}^2\rangle, \quad (8)$$

where η^2 is the factor by which the average of the squares of the measurement errors should be incremented. For various assumed values of η we calculated the average of Q for the entire set of the 74 DLCs, as well as the numbers of DLCs for which Q was found to be positive and negative, respectively. The condition of the mean value of Q being equal to zero (i.e. $\langle Q\rangle = 0$), is satisfied for $\eta = 1.55$. On the other hand, the median value of Q is zero for $\eta = 1.40$. Thus, we adopt a value of $\eta = 1.50$ in further analysis. Note that this value is somewhat lower than 1.75 estimated in Gopal-Krishna *et al.* (1995) and the 1.73 reported by Garcia *et al.* (1999).

6. Optical variability

In all, 113 nights of observations were carried out; however, the data on 5 of these nights were found to be too noisy for the purpose of searching for INOV, and hence were used only for long term optical variability (LTOV) measurements (section 6.2). The basic statistics on the detection of INOV for the different AGN classes are summarized in Table 3. The DLCs for a total of 42 nights of observations (8 for RQQs, 10 for LDQs, 6 for CCQs, and 18 for BL Lacs) have already been reported in SGSW04 and SSGW04. Here we present, in Fig. 5, the DLCs for the remaining 66 nights of observations, covering 7 RQQs (21 nights), 7 LDQs (27 nights), 4 CDQs (10 nights) and 4 BL Lacs (8 nights).

Table 3. Statistics on the detection of INOV for different AGN classes. The number of sources (N_s) monitored on N_o nights during N_d hours showed INOV in N_i sources during N_{ni} nights for N_{di} hours. The corresponding numbers are given in 2nd, 4th, 5th, 3rd, 6th and 7th columns respectively.

Type	N_s	N_i	N_o	N_d	N_{ni}	N_{di}	DC* (%)	$\langle\delta_{\rm obs}\rangle^\dagger$
RQQ	7	3	29	185	5	28	17	1.19
LDQ	8	4	37	218	7	48	12	1.62
CDQ	5	1	16	107	4	29	20	1.47
BL	6	6	26	172	17	119	61	1.96
Total	26	14	108	682	33	224		

*Duty cycle.
†Mean of the Doppler factors for that group.

6.1 *Intra-night optical variability*

This observing programme has led to the first clear detection of INOV in RQQs (see GSSW03), with additional data supporting this important result presented in SGSW04 and in Tables 2 and 3. A clear distinction between the INOV nature of the two classes of presumably relativistically beamed radio-loud AGNs (CDQs and BL Lacs) is found for the first time, in the sense that BL Lacs are certainly more frequently variable than are CDQs (SSGW04); this is also clear from Table 3.

To make a claim of INOV in a given night, we have employed a statistical criterion based on the parameter C, similar to that followed by Jang & Miller (1997), with the added advantage that for each AGN we have DLCs relative to multiple comparison stars. This allows us to discard any variability candidates for which the multiple DLCs do not show clearly correlated trends, both in amplitude and time. We define C for a given DLC as the ratio of its standard deviation, σ_T, and the mean σ of its individual data points, $\eta\sigma_{\rm err}$. This value of C_i for the ith DLC of the AGN has the corresponding probability, p_i, that the DLC is steady (non-variable), assuming a normal distribution. For a given AGN on a given night we then compute the joint probability, P, by multiplying the values of p_i's for the individual DLCs available for the AGN. We consider a quasar to be variable if $C_{\rm eff} > 2.57$, which corresponds to a confidence level of variability in excess of 99%. A quasar is occasionally classified as a probable variable (PV) if $2.57 \geq C_{\rm eff} > 2.00$, giving rise to a confidence level between 90% and 99%. The values of $C_{\rm eff}$ for variable and probable variable quasars along with the nightly variability status of each of the quasars monitored in this program are given in Table 2.

To quantify the variability amplitude of a DLC we adopt the commonly used definition (e.g., Heidt & Wagner 1996; Romero *et al.* 1999)

$$\psi = \sqrt{(D_{\rm max} - D_{\rm min})^2 - 2\sigma^2}, \tag{9}$$

where $D_{\rm max}$, $D_{\rm min}$ are the maximum and minimum in the quasar differential lightcurve relative to a stable star and $\sigma^2 = \eta^2\langle\sigma_{\rm err}^2\rangle$. By subtracting off (in quadrature) the corrected errors from the total variability, this expression for ψ gives a fairer estimate of the true amplitude of variability. We have found the correction factor $\eta \simeq 1.50$ (see section 5.3). The values of ψ for quasars showing INOV are given in Table 2. A key result is that all 4 types of luminous AGN do sometimes exhibit INOV when observed

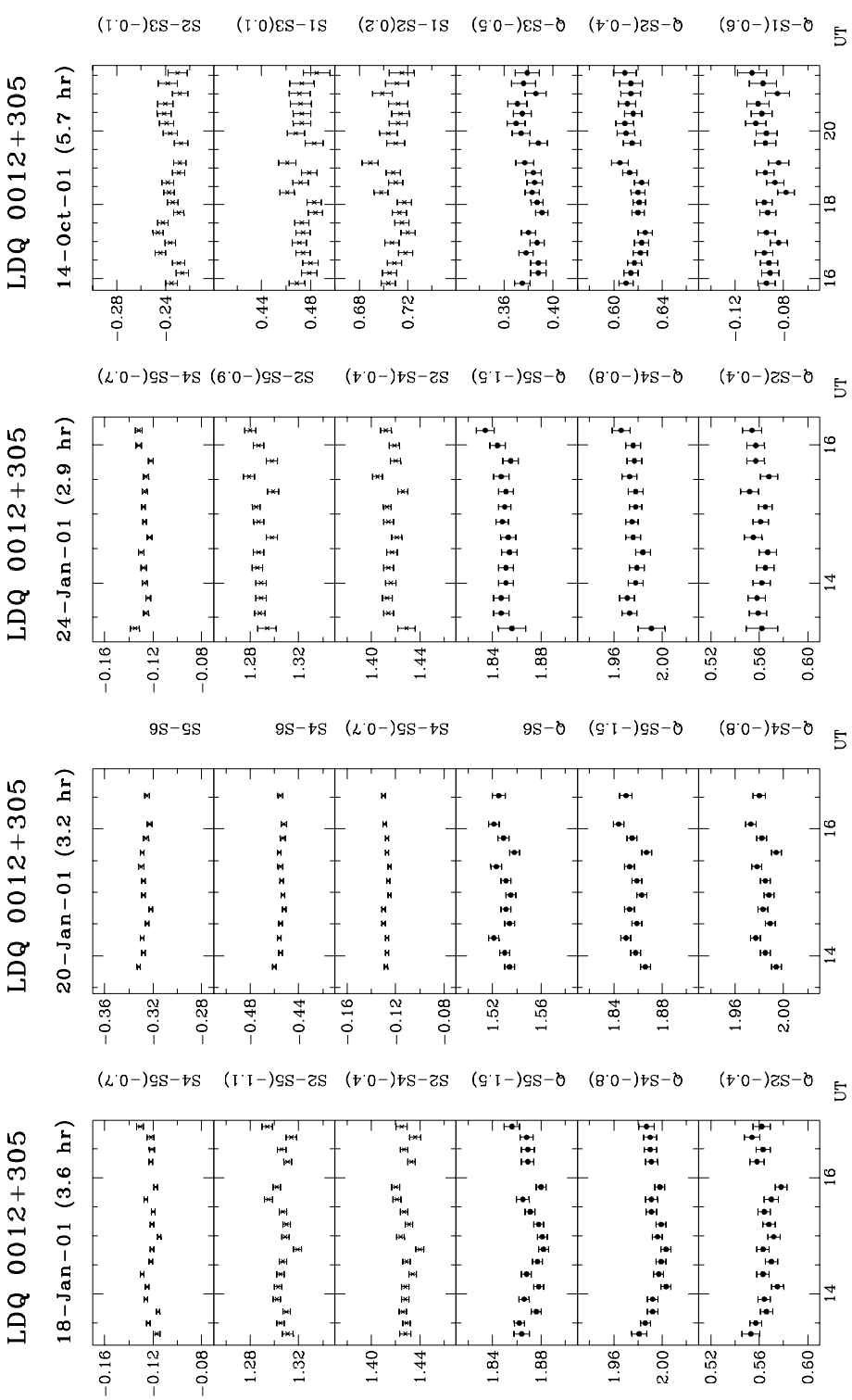

Figure 5. (*Continued*)

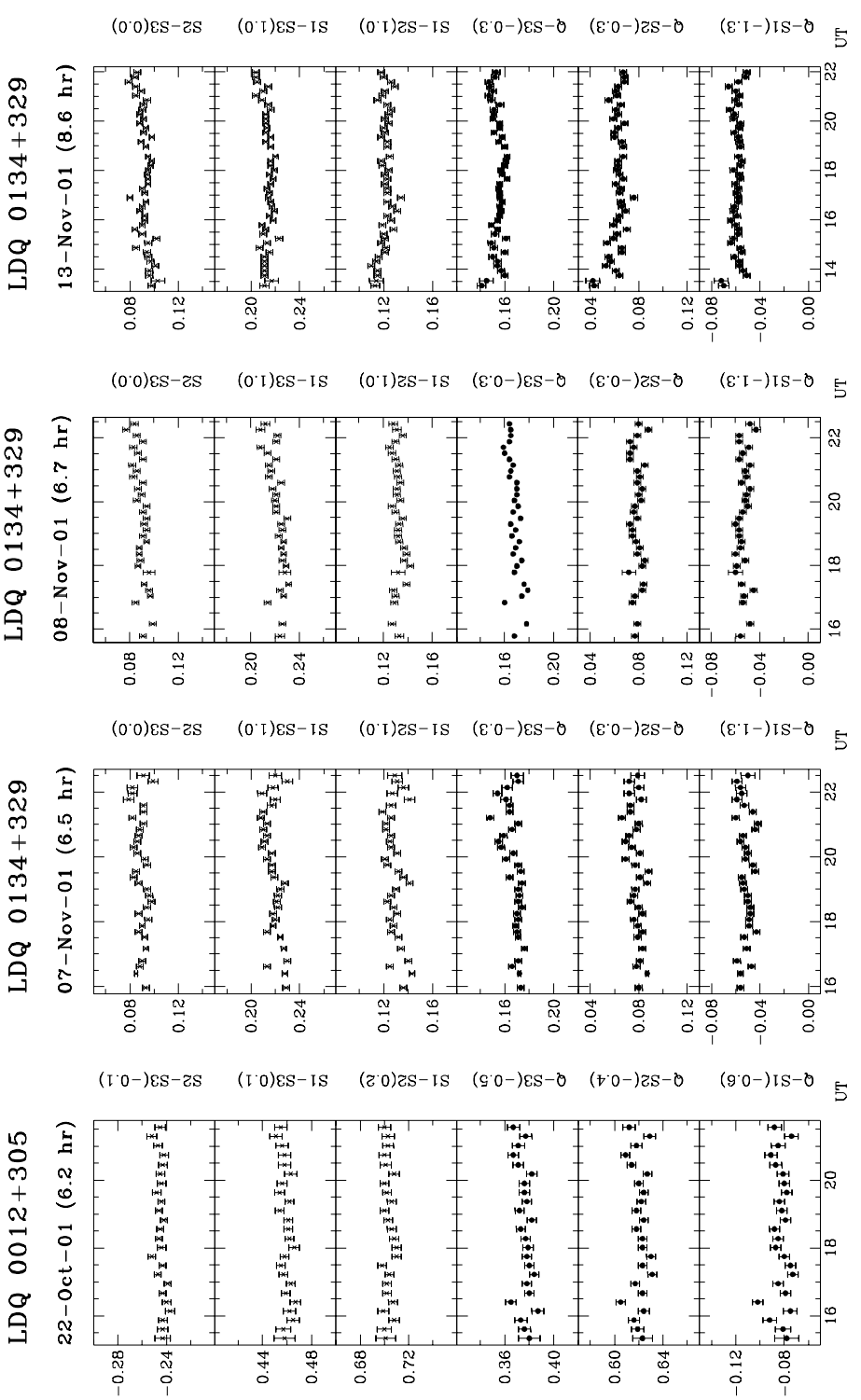

Figure 5. (*Continued*)

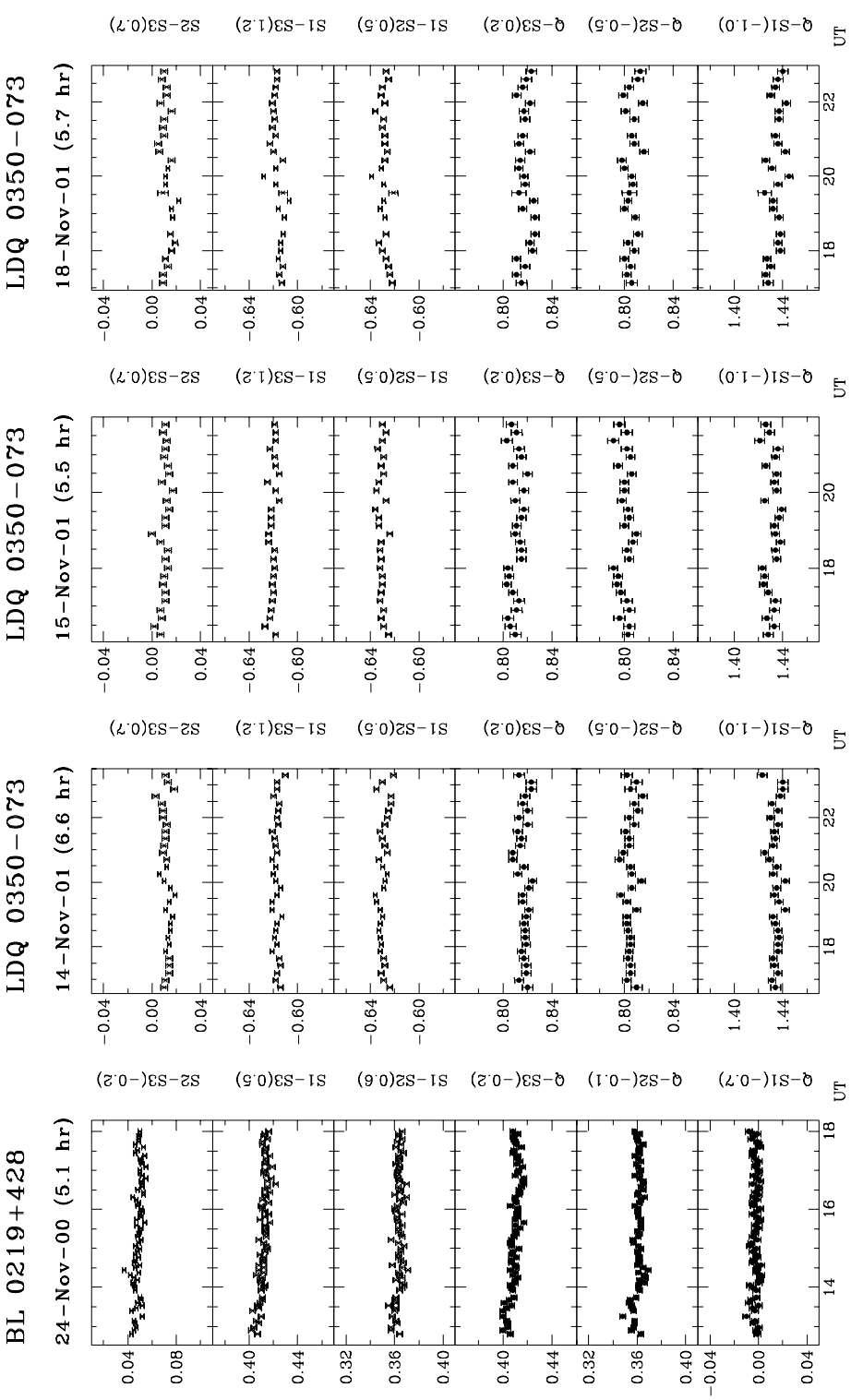

Figure 5. (*Continued*)

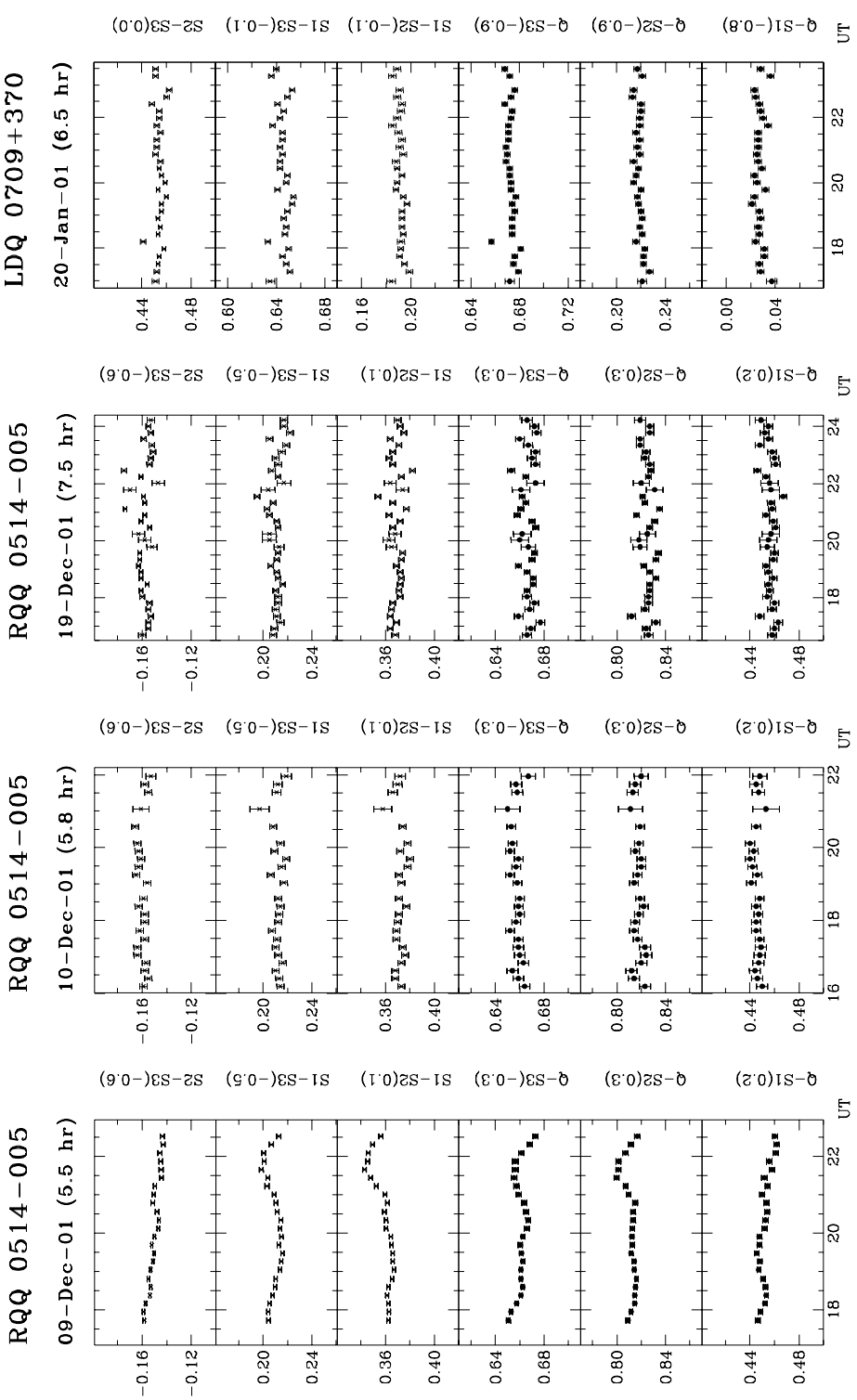

Figure 5. (*Continued*)

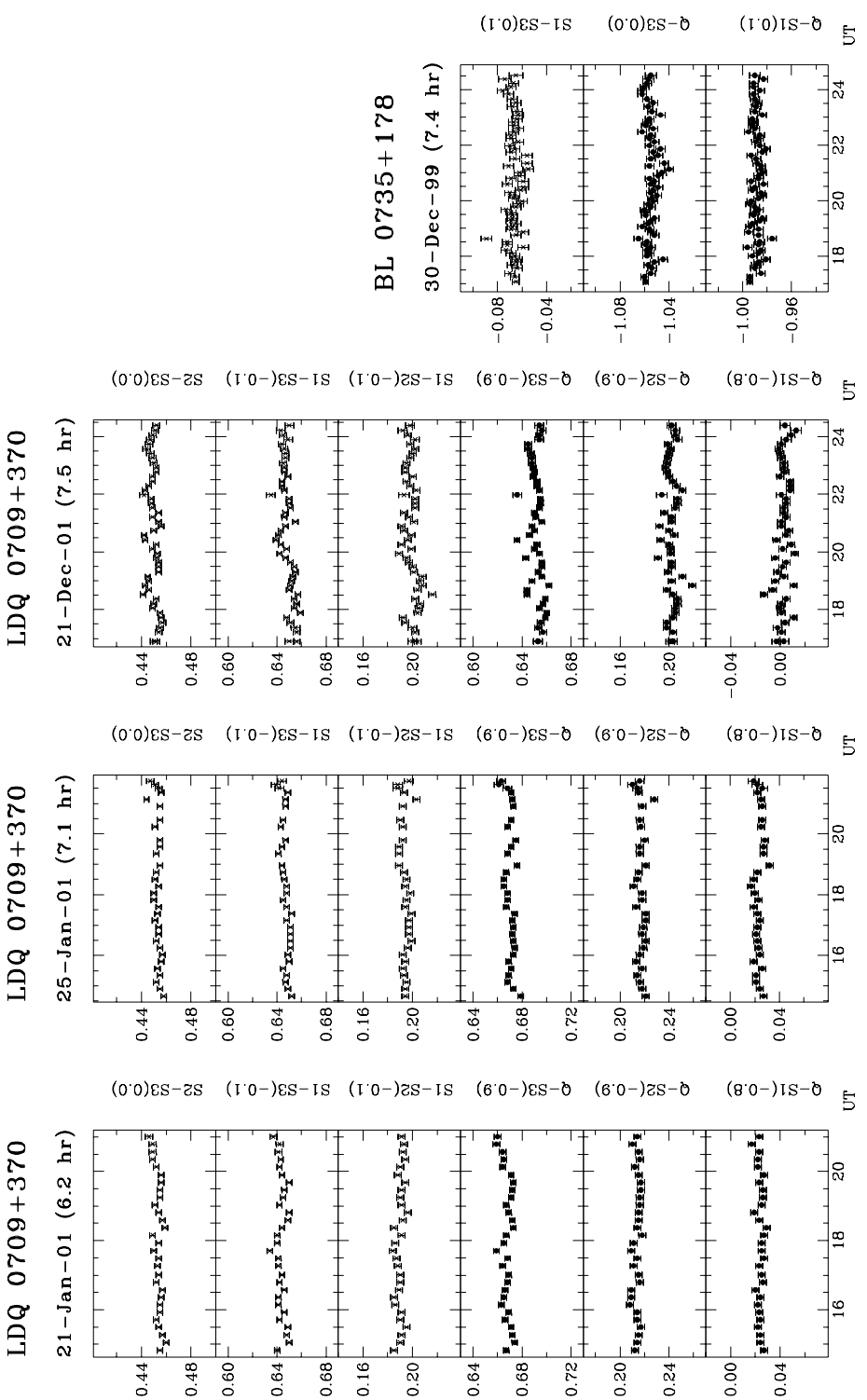

Figure 5. (*Continued*)

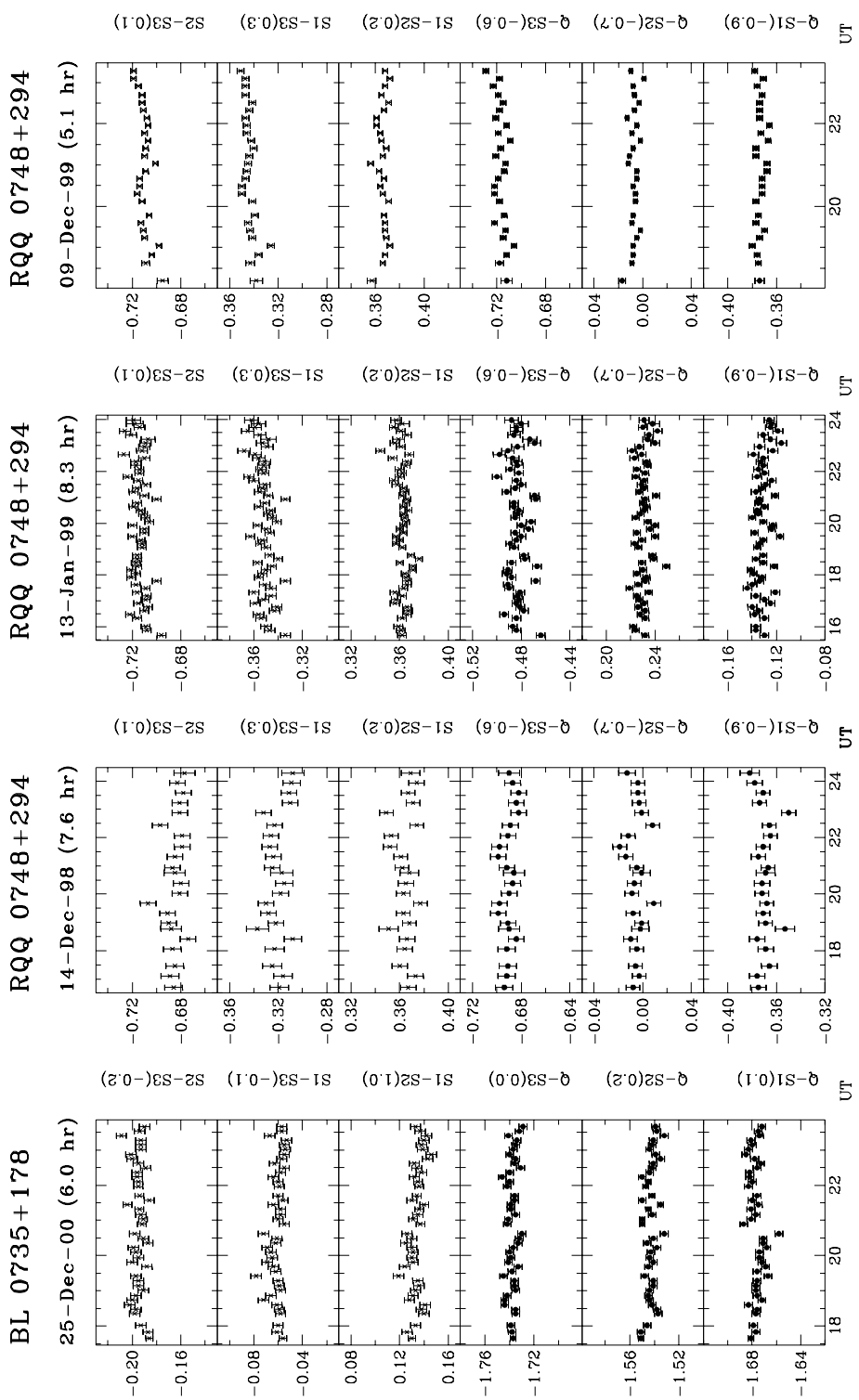

Figure 5. (*Continued*)

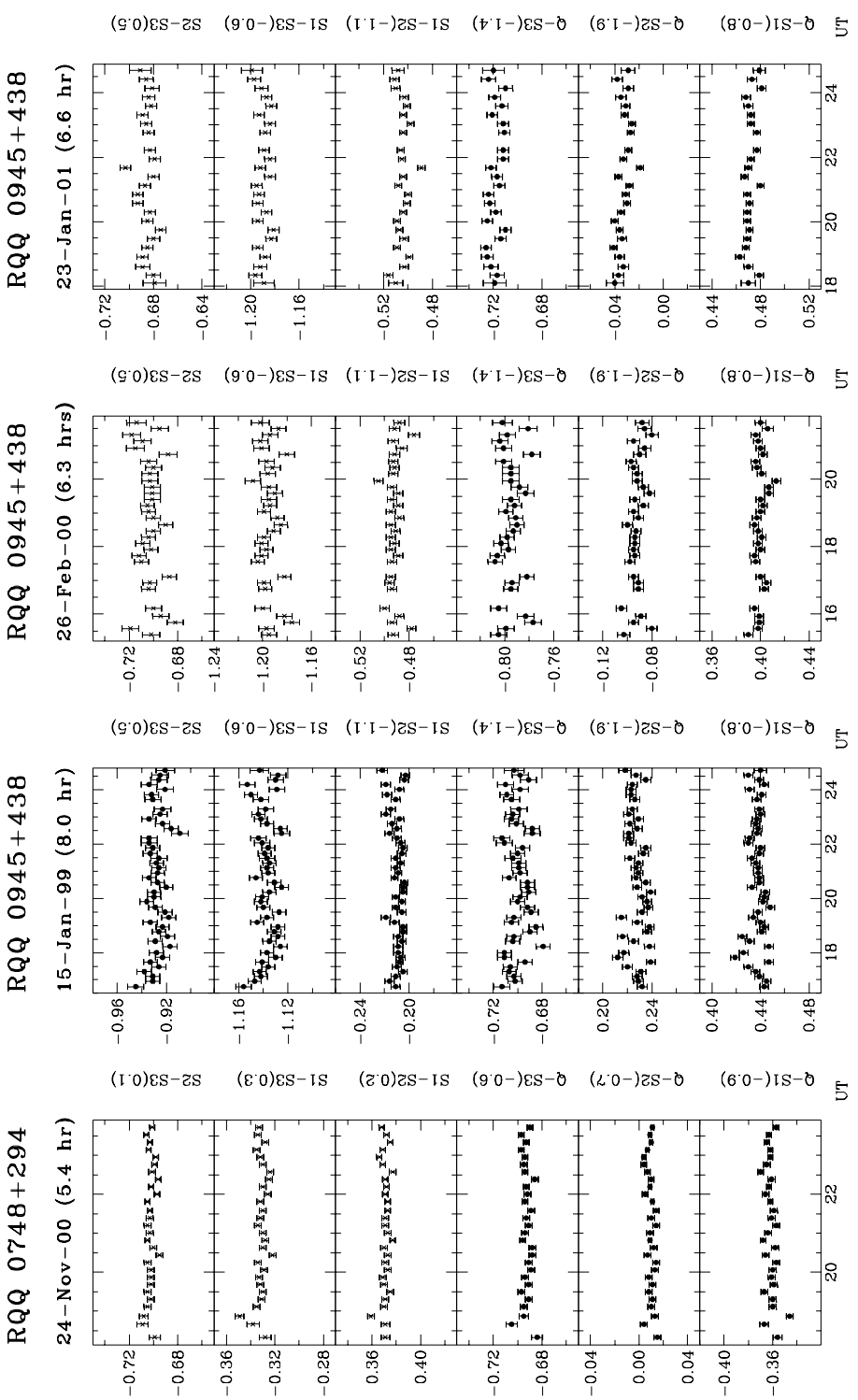

Figure 5. (*Continued*)

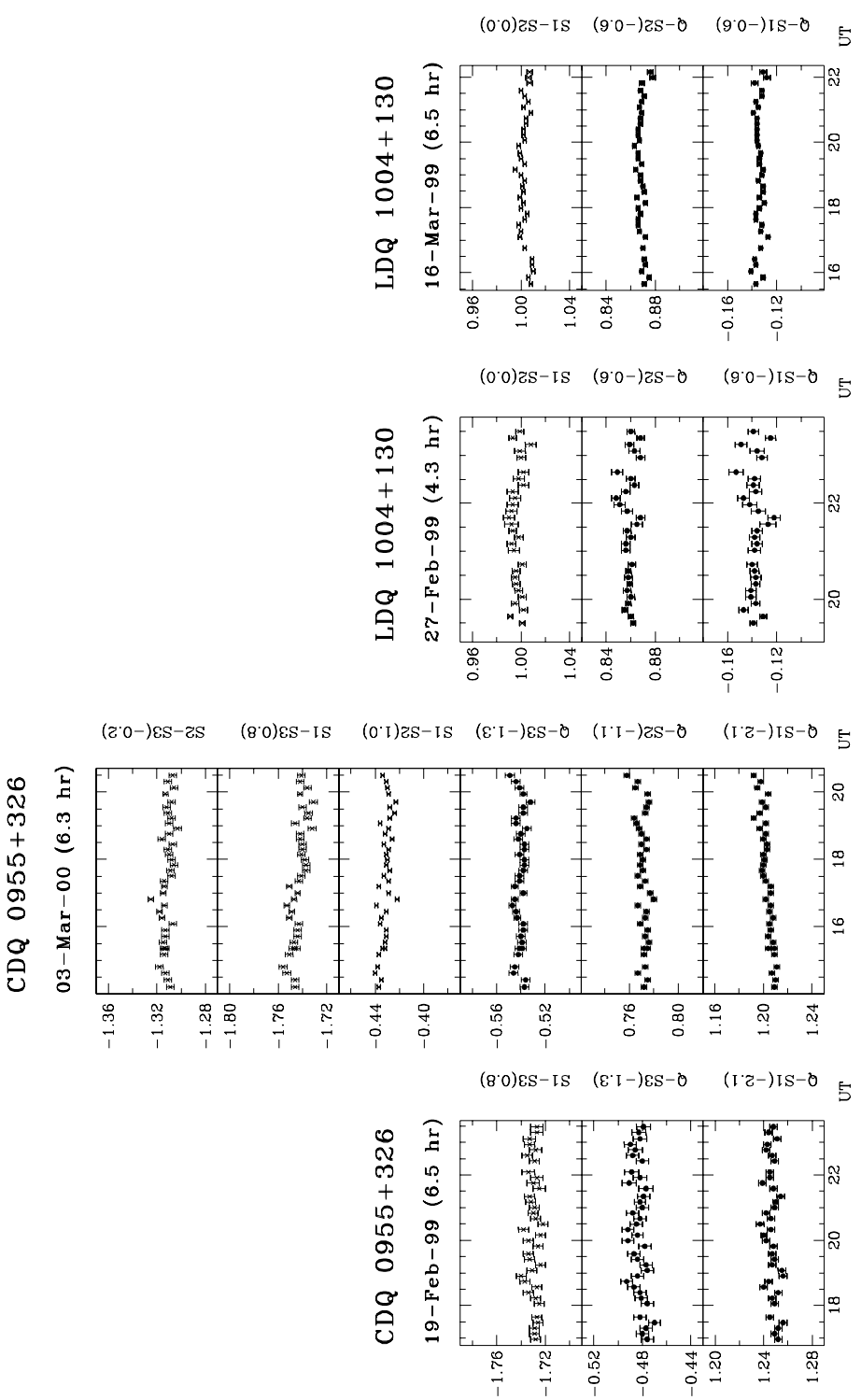

Figure 5. (*Continued*)

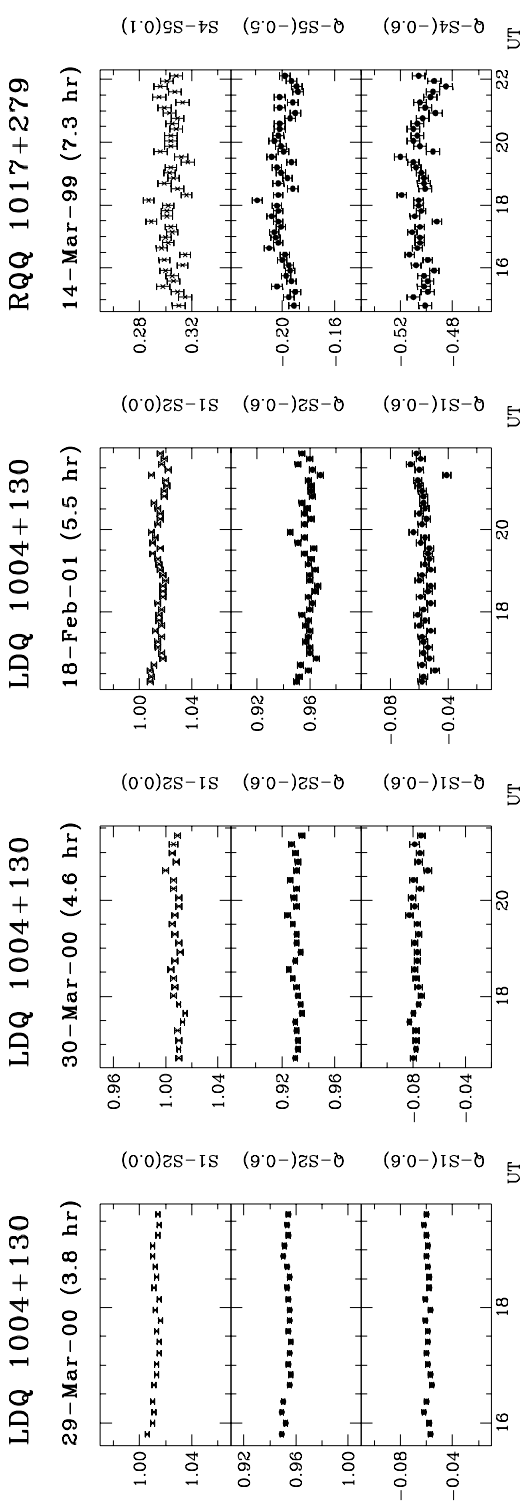

Figure 5. (*Continued*)

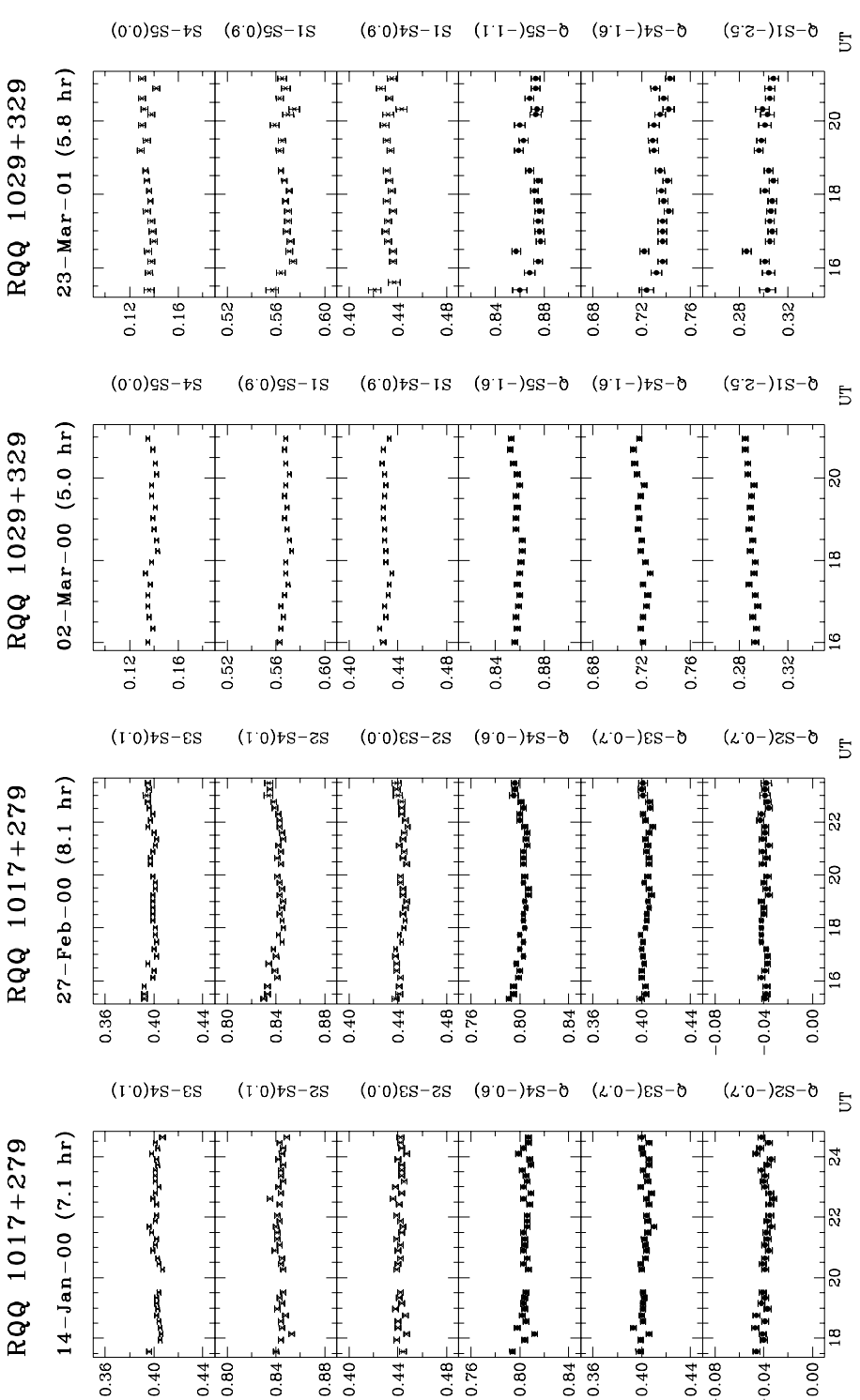

Figure 5. (*Continued*)

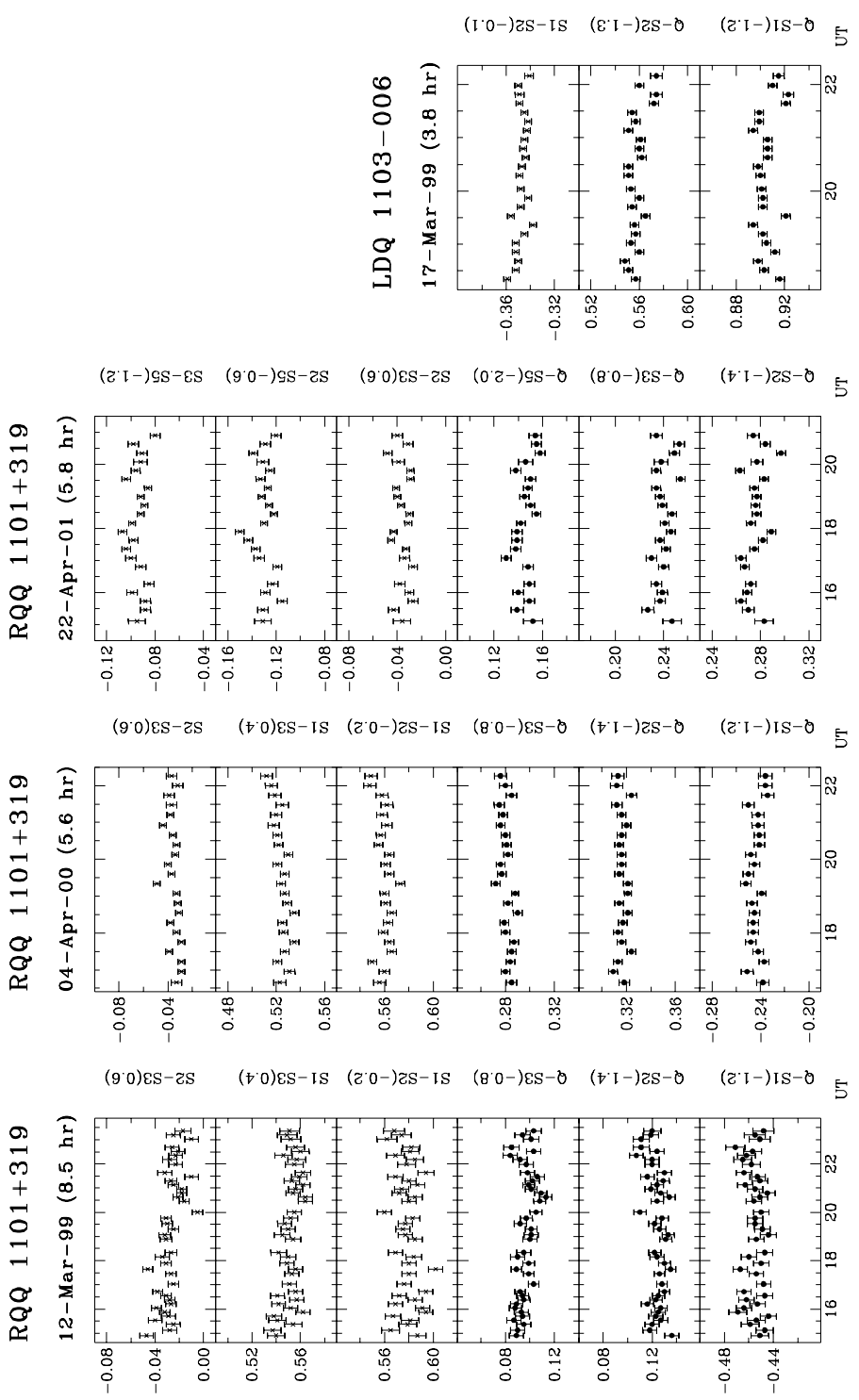

Figure 5. (*Continued*)

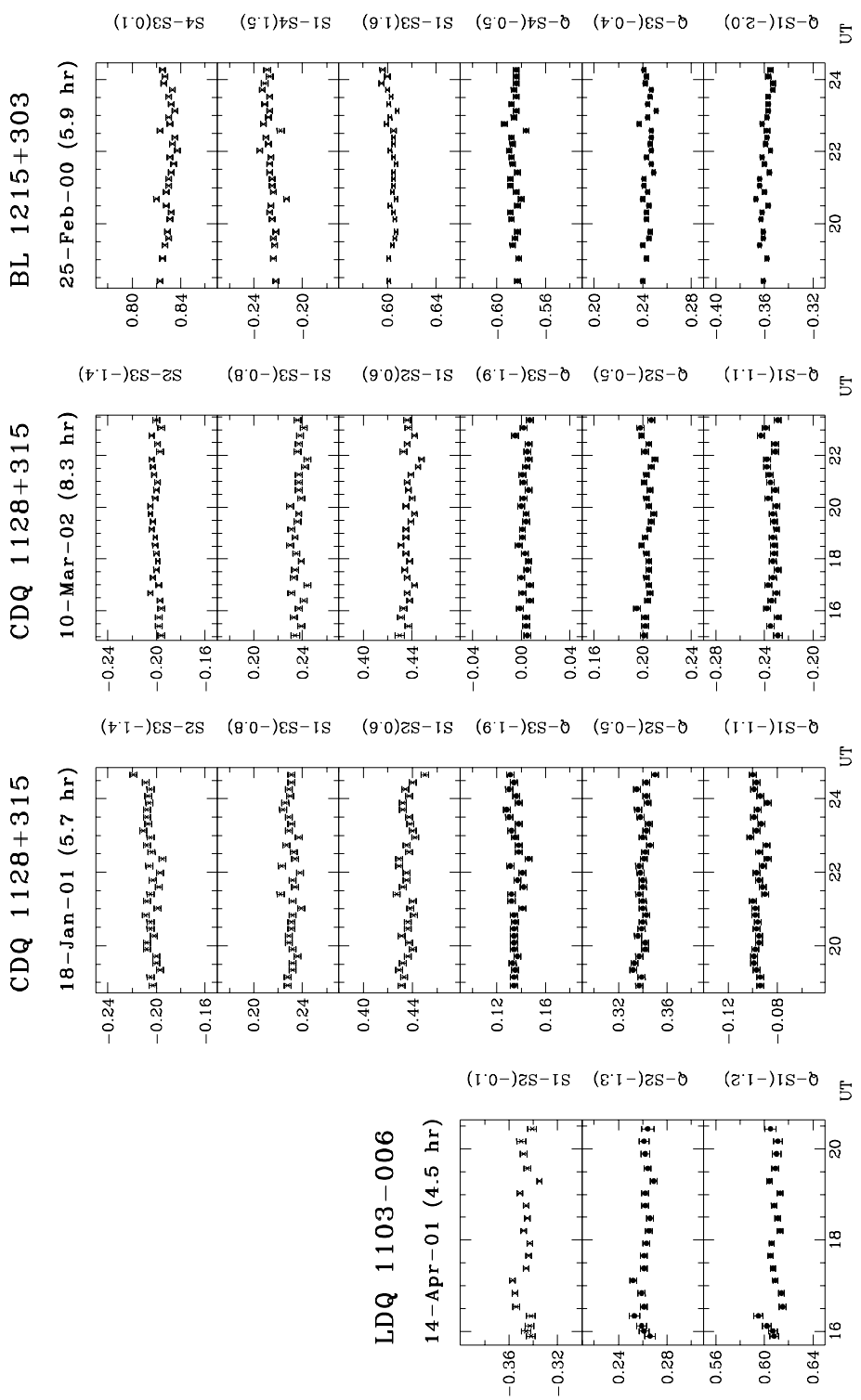

Figure 5. (*Continued*)

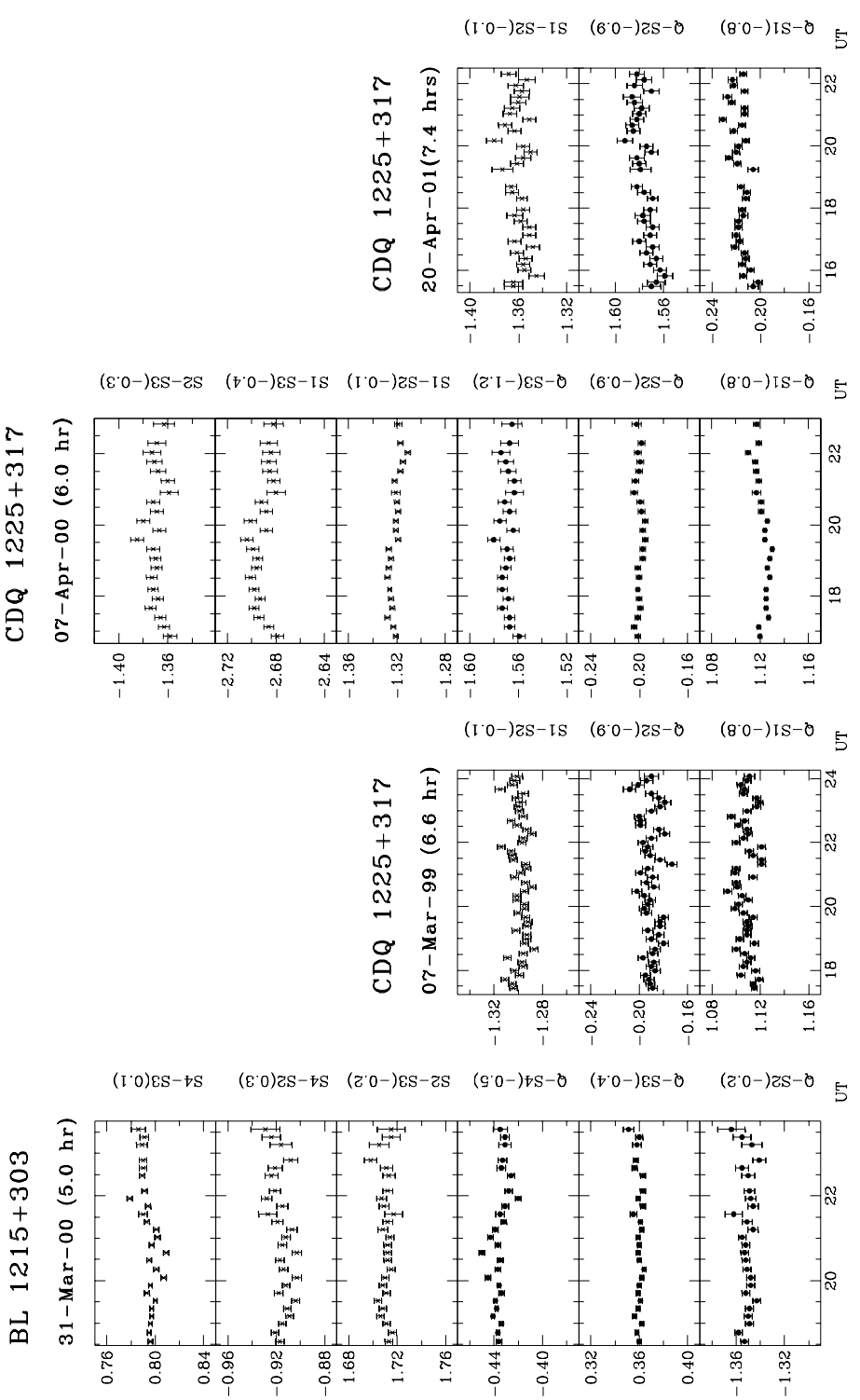

Figure 5. (*Continued*)

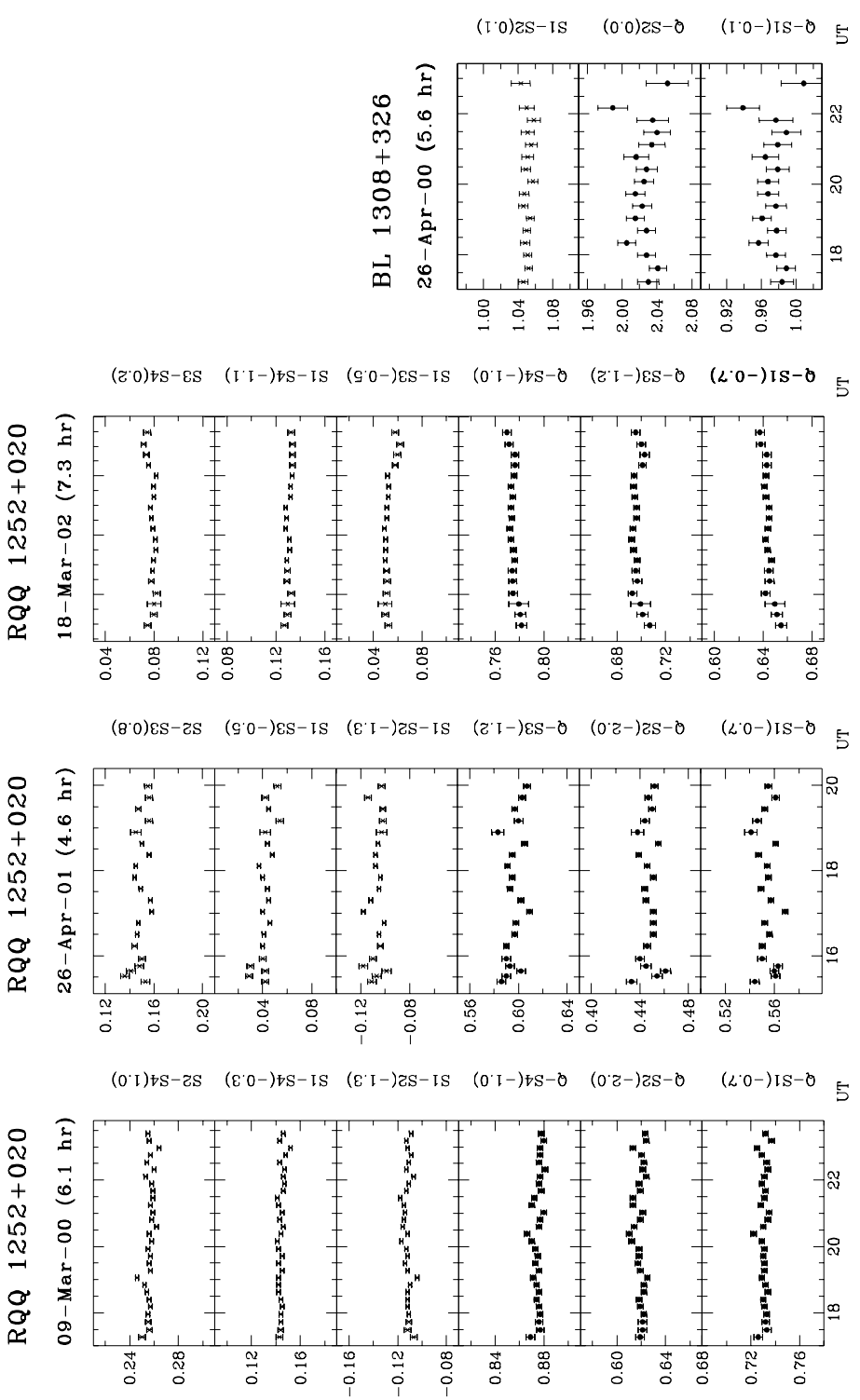

Figure 5. (*Continued*)

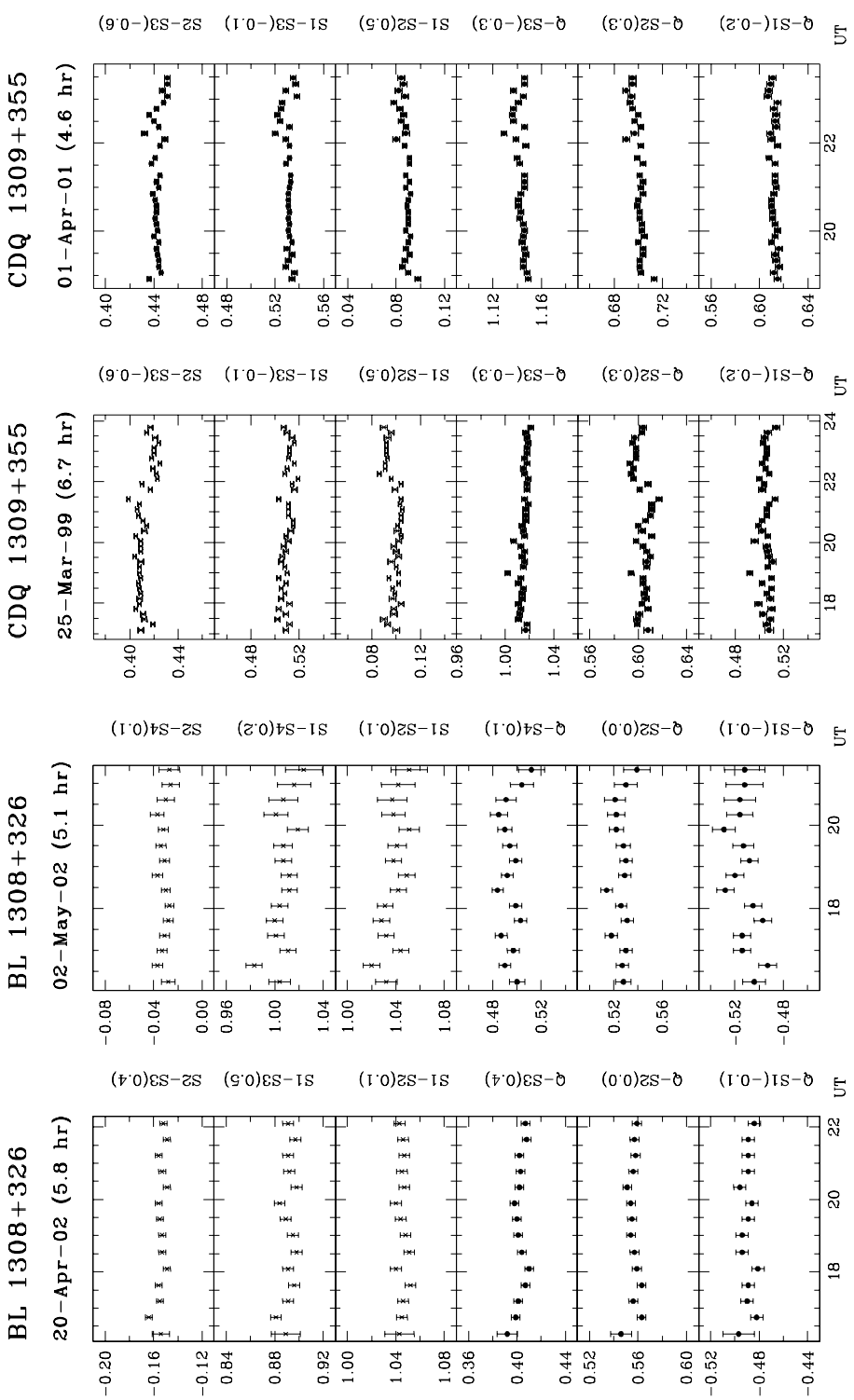

Figure 5. (*Continued*)

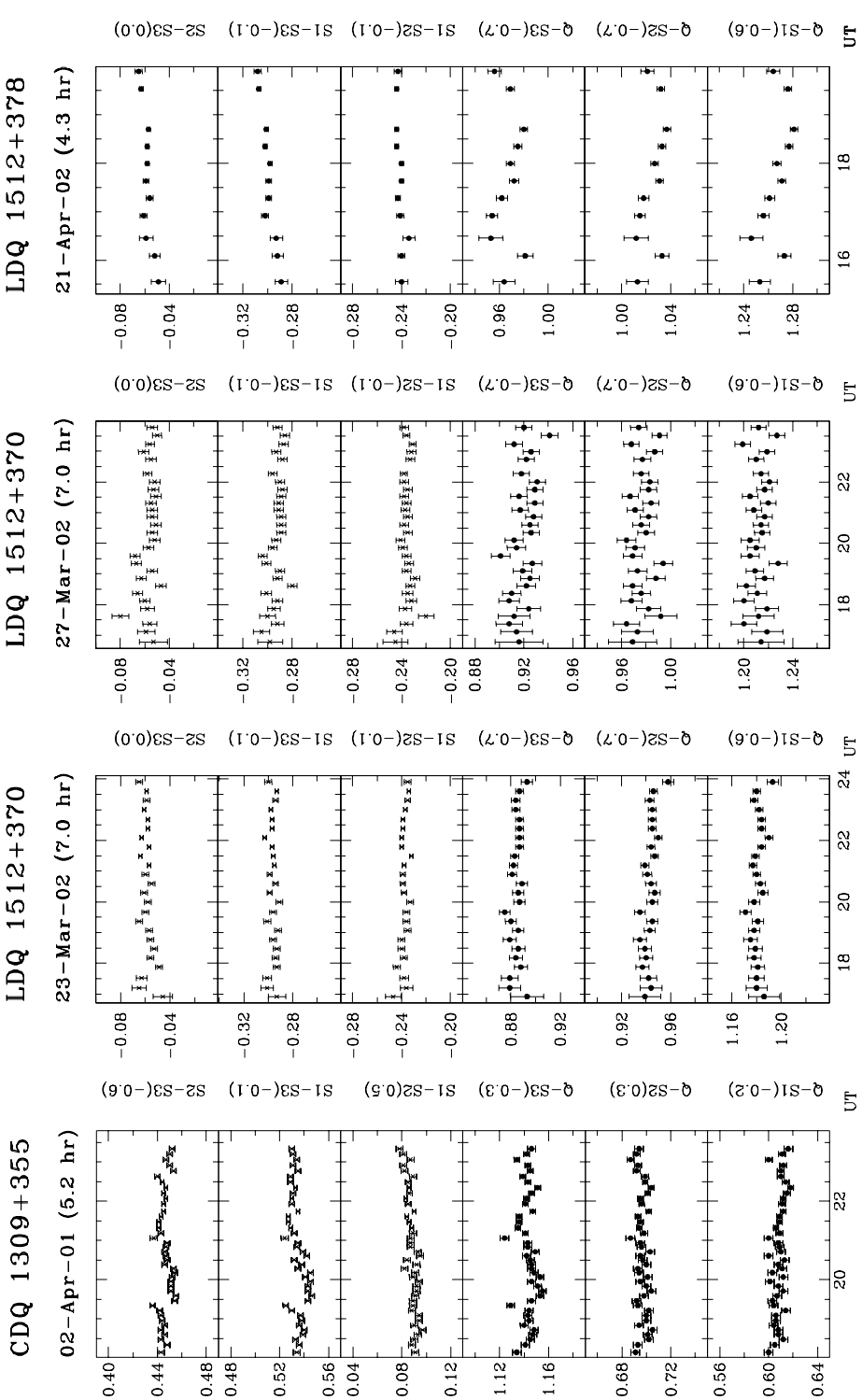

Figure 5. (*Continued*)

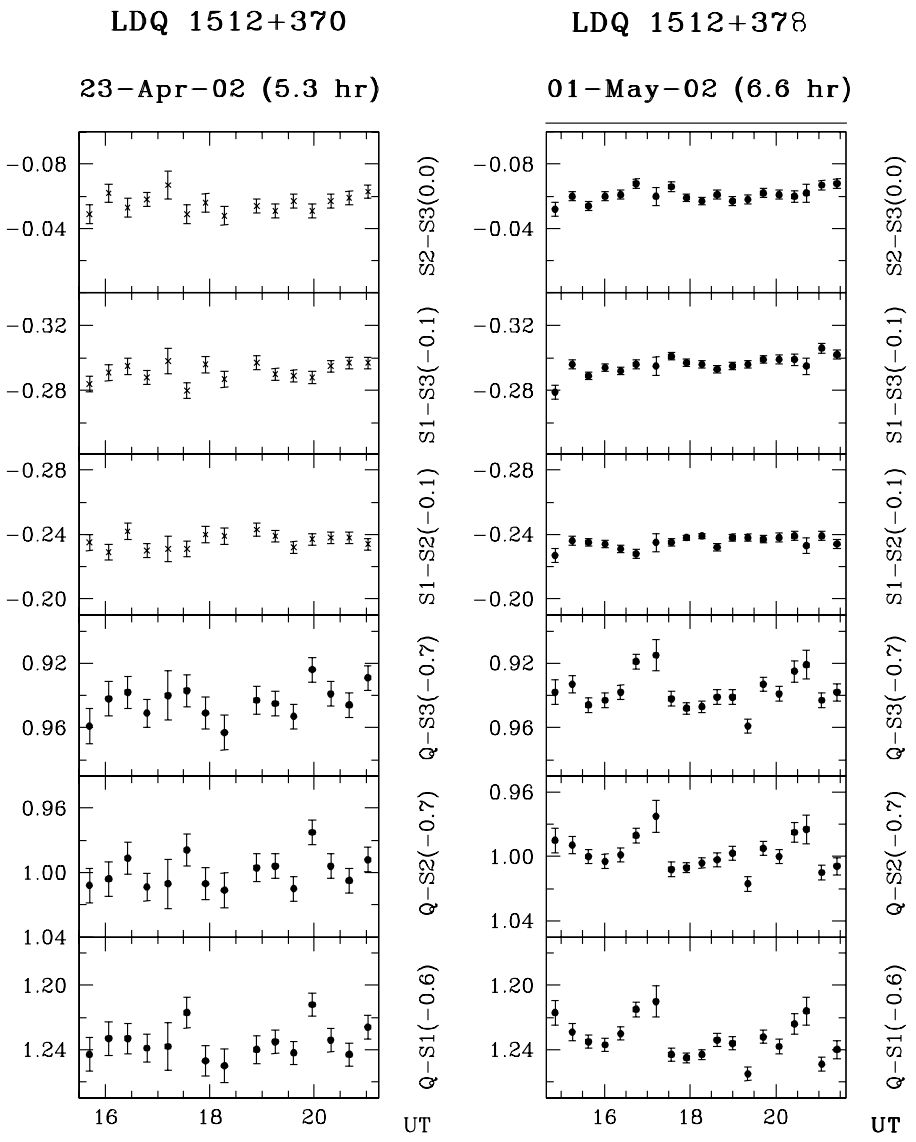

Figure 5. Differential R-band lightcurves of the different types of quasars. The name of the object, the date and duration of observations in hours are given on the top of each panel. The objects being compared and their colour differences (in parentheses) label the right side of each sub-panel.

carefully, but that BL Lacs show far large values of ψ much more frequently (see SSGW04).

6.1.1 *Structure function analysis*

Structure function (SF) analysis is a useful pointer to the variability characteristics of the lightcurves, such as the time-scales and possible periodicities. The general

definition of SF and associated properties are described, e.g., by Simonetti *et al.* (1985), and Hughes, Aller & Aller (1992), Heidt & Wagner (1996). Following Simonetti *et al.* (1985) we have defined the first-order SF as

$$D_X^1(\tau) = \frac{1}{N(\tau)} \sum_{i=1}^{N} [X(i+\tau) - X(i)]^2, \tag{10}$$

where τ = time lag, $N(\tau) = \sum w(i)w(i+\tau)$, and the weighting factor $w(i) = 1$ if a measurement exists for the ith interval, and 0 otherwise. The error in each point in the computed SF is

$$\sigma^2(\tau) = \frac{8\sigma_{\delta X}^2}{N(\tau)} D_X^1(\tau), \tag{11}$$

where $\sigma_{\delta X}^2$ is the measured noise variance.

Since the sampling of our DLCs is quasi-uniform, we have determined the SFs using an interpolation algorithm. For any time lag τ, the value of $X(i+\tau)$ was calculated by linear interpolation between the two adjacent data points. A typical time scale in the light curve (i.e., time between a maximum and a minimum, or vice versa) is indicated by a local maximum in the SF. In the case of a monotonically increasing SF, the source possesses no typical time-scale smaller than the total duration of observations. A minimum in the SF is an indication of periodicity. The SF plots for 1 CDQ and 6 BL Lacs which showed definite INOV during 21 nights of observation are given in SSGW04. Here in Fig. 6, we present SF plots for 3 RQQs and 3 LDQs which showed confirmed INOV during 10 nights of observations. The inferred variability timescale(s) and "period"(s) are given in Table 2. Because none of our light curves were long enough to show more than two maxima or minima, it should be stressed that we are not claiming that we detect actual periodic component of the INOV in any of our sources. Because the SFs for individual sources are usually different from night to night, the chance that any nominal "periods" detected in the SFs are of physical origin is further reduced.

6.1.2 *Duty cycles of intra-night optical variability*

The high precision of our data permit the estimation of INOV duty cycle (DC) not only for different AGN classes, but also for different levels of INOV amplitudes. The DC of INOV of a given class of objects is given by (Romero *et al.* 1999)

$$DC = 100 \frac{\sum_{i=1}^{n} N_i (1/\Delta t_i)}{\sum_{i=1}^{N} (1/\Delta t_i)} \ \%, \tag{12}$$

where $\Delta t_i = \Delta t_{i,\mathrm{obs}}(1+z)^{-1}$ is the duration (corrected for cosmological redshift) of the ith monitoring session of the source in the selected class. N_i equals 0 or 1, depending on whether the object was respectively, non-variable, or variable during Δt_i.

A DC of 17% was found for RQQs considering only sessions for which INOV was unambiguously detected. This value is roughly midway between the lower values published by Jang & Miller (1997) and Romero *et al.* (1999) and the higher estimate of de Diego *et al.* (1998). For LDQs, a DC of only $\sim$ 12% is found for clear detection

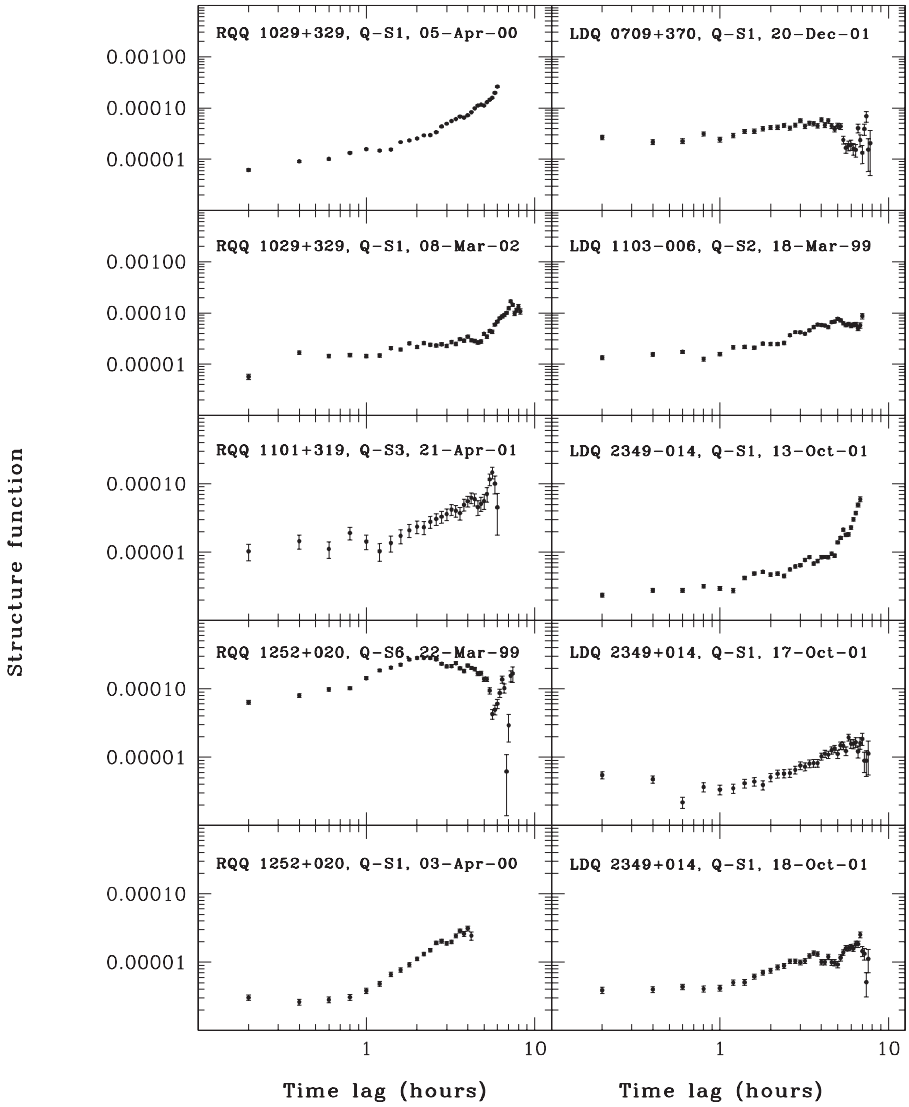

Figure 6. First order structure function of RQQs (left panels) and LDQs (right panels) which have shown INOV, given in increasing order of right ascension.

of INOV; however, this rises to about 18% if the two cases of probable detection are included. Also, a distinction is found in DCs between the two presumably relativistically beamed AGN classes, namely BL Lacs and CDQs. BL Lacs are found to show a high DC, $\sim 61\%$, whereas CDQs show a DC of only $\sim 20\%$. These results are summarised in Table 3. However, separating the CDQs into high polarization (CDQ-HP) and low polarization (CDQ-LP) subsets may be relevant, although we stress that there is only one CDQ-HP in the sample ($1216-010$) and only 4 CDQ-LPs; CDQ-LPs show very low DC ($< 10\%$), whereas a much higher value of DC is found for the single CDQ-HP source (100%). It thus appears that INOV may be more closely connected

to high optical polarization than to Doppler boosting *per se*. Such polarized emission is commonly attributed to shocks in relativistic jets (see SSGW04 for additional discussion).

6.1.3 *Relativistic beaming, Doppler factors, and accretion efficiency*

We have estimated the observed Doppler factor ($\delta_{\rm obs}$) and accretion efficiency ($\eta_{\rm obs}$) for our dataset within the framework of the relativistic beaming models (e.g., Marscher & Scott 1980). The apparent R magnitudes of the quasars (m_R) were obtained from their observed DLCs using the apparent R magnitudes of the comparison stars given in USNO catalog. These were converted to observed monochromatic fluxes (S_R) following Bessel (1979) as

$$S_R = 3.08 \times 10^{-23} 10^{-0.4 m_R} \quad \text{W m}^{-2}\text{Hz}^{-1}. \tag{13}$$

The rest-frame observed monochromatic luminosity of the source at frequency ν_o (which we take as the frequency corresponding to the V-band)

$$L_{\nu_o} = 4\pi \left(\frac{cz}{H_o}\right)^2 \left(1 + \frac{z}{2}\right)^2 S_{\nu_o} \qquad \text{for} \quad q_o = 0, \tag{14}$$

where

$$S_{\nu_o} = S_{\nu_{\rm obs}} \left[\frac{\nu_o}{\nu_{\rm obs}(1+z)}\right]^{\alpha} (1+z)^{-1}, \tag{15}$$

and where $\nu_{\rm obs}$ = frequency corresponding to R-band, $S_{\nu_{\rm obs}}$ = flux observed in R-band, and $\alpha = d(\ln S)/d(\ln \nu)$; we take $\alpha = -1$ which is typical for the spectra of quasars in the visible band.

The observed bolometric luminosity is then calculated from this monochromatic luminosity, using the scaling factor given by Elvis *et al.* (1994) for V-band as

$$L_{Bol}/L_V = 13.2, \tag{16}$$

where $L_V = \nu L_\nu$ at V-band ($\nu = 5.456 \times 10^{14}$ Hz) (Elvis *et al.* 1994).

We have defined $\Delta t_{\rm min}$ as the minimum variability time-scale observed for a clearly detected fluctuation on a given night, corrected to the intrinsic value in the source frame, by dividing the observed $\Delta t_{\rm obs}$ by $(1+z)$. Luminous outbursts of energy ΔL (ergs s^{-1}), cannot occur on time-scales, $\Delta t_{\rm min}$, much shorter than the light crossing time of the emitting region. In this case, the inferred efficiency ($\eta_{\rm obs}$) for the conversion of accreted matter into energy for the case of spherical, homogeneous, non-relativistically beamed co-moving emitter is given as (Fabian & Rees 1979)

$$\eta_{\rm obs} \geq 5 \times 10^{-43} \Delta L / \Delta t_{\rm min}. \tag{17}$$

Assuming that the bolometric luminosity also changes in the same manner as does the flux during the outburst (e.g., Zhang, Fan & Cheng 2002), we have estimated $\eta_{\rm obs}$, taking ΔL to be the variable fraction of the bolometric luminosity during $\Delta t_{\rm min}$.

It is commonly accepted that the immense energy production in AGN is due to accretion onto black holes (BHs). The efficiency of conversion of mass to energy

through that accretion via thin disks is typically taken as 0.057 for non-rotating BHs but can range up to 0.32 for rapidly rotating black holes (e.g., Paczyński & Wiita 1980; Frank, King & Raine 1986). However, if the accretion is essentially spherical (a Bondi flow) or radiatively inefficient then the efficiency factor can be considerably lower (e.g., Quataert & Narayan 1999). We have calculated the lower limit of $\eta_{\rm obs}$ for all the quasars in our sample which show definite variability and the results are given in Table 2. If $\eta_{\rm obs}$ is found to be greater than 0.1, relativistic beaming is usually invoked to explain the observations.

Once $\eta_{\rm obs}$ has been estimated, one can calculate self-consistent (though clearly somewhat arbitrary, thanks to the several assumptions made in this subsection) limits on $\delta_{\rm obs}$. We have $\Delta L({\rm obs}) = \delta_{\rm obs}^{3+\alpha} \Delta L(int)$ and $\Delta t_{\rm min}({\rm obs}) = \delta_{\rm obs}^{-1} \Delta t_{\rm min}(int)$, where (int) refers to intrinsic quantities (Worrall 1986; Frank, King & Raine 1986). If we employ Equation (17) as an equality so as to provide a lower bound, $\eta_{\rm obs} = 5 \times 10^{-43} \Delta L({\rm obs})/\Delta t_{\rm min}({\rm obs})$, we then find $\eta_{int} = 5 \times 10^{-43} \Delta L(int)/\Delta t_{\rm min}(int)$, and thus

$$\delta_{\rm obs} \geq (\eta_{\rm obs}/\eta_{int})^{1/(4-\alpha)}. \tag{18}$$

If η_{int} is assumed to be known, a lower bound to $\delta_{\rm obs}$ can now be calculated. We assume a conservative value of $\eta_{int} = 0.05$, which is almost equal to the value of 0.057 derived from non-rotating BH thin accretion disk theory (e.g., Paczyński & Wiita 1980) in estimating δ. The derived $\delta_{\rm obs}$ lower bounds for all the variable objects with $\eta_{\rm obs} \geq 0.1$ in our sample are given in Table 2. The average and median values of $\eta_{\rm obs}$ are 0.89 and 0.33 respectively, while $\delta_{\rm obs}$ range between 1 and 2.55 with both a mean and a median of 1.6.

Only 2 RQQs ever showed $\eta_{\rm obs} > 0.1$ and both just barely did so. Only 1 LDQ had such high variability (on just one occasion); similarly, only 1 CDQ showed high variability, but did so on three nights. In contrast, 5 of 6 BL Lacs evinced $\eta_{\rm obs} > 0.1$, most on more than one occasion. The mean values of these lower bounds to $\delta_{\rm obs}$ for the different classes of AGN are tabulated in the last column of Table 3. As would be expected for the unification scheme, the values for BL Lacs are highest and those for RQQs are lowest. We stress that this computation produces only lower bounds to δ and most estimates of δ for blazars as obtained from Very Long Baseline Interferometry are somewhat higher (e.g., Kellermann *et al.* 2004).

6.2 *Long term optical variability*

Long term optical variability (LTOV) is seen in 20 out of 26 objects in our sample during the period of our observations. The number of epochs covered range between three and seven and the total time span covered range between about a week to three years. Table 4 presents the LTOV results for our sample. This was quantified by identifying at least one stable ('well behaved') comparison star common to all the epochs and then calculating the mean optical magnitude of the quasar relative to that star for each epoch. The night for which the quasar had the minimum optical brightness is taken as the base level for LTOV and the resulting offset values of the quasars magnitudes are given in Table 4, in the sequence of increasing brightness. Thus, these data provide a decent quantitative description of the LTOV of the quasars. It may, however, be noted that due to the scheduling constraints, the total time span covered is highly variable from quasar to quasar, as can be seen from our log of observations in Table 2. The

Table 4. Results for Long Term Optical Variability of the QSOs.

Object	Type	Date	Q-S1 (mag)	Q-S2 (mag)	Q-S3 (mag)	S1-S2 (mag)	S1-S3 (mag)	S2-S3 (mag)
2349−014	LDQ	17.10.01	0.000	0.000	0.000	0.000	0.000	0.000
		13.10.01	0.030	0.035	0.047	0.005	0.016	0.011
		18.10.01	0.046	0.048	0.049	0.002	0.002	−0.001
1309+355	LDQ	01.04.01	0.000	0.000	0.000	0.000	0.000	0.000
		02.04.01	0.004	0.003	0.000	0.000	−0.004	−0.004
		25.03.99	0.107	0.097	0.128	−0.010	0.021	0.031
1215+303	BL	25.04.01	0.000		0.000			0.000
		19.04.01	0.108		0.098			−0.010
		31.03.00	0.201		0.206			0.006
		25.02.00	0.344		0.322			−0.022
		20.03.99	0.522		0.468			−0.054
0514−005	RQ	19.12.01	0.000	0.000	0.000	0.000	0.000	0.000
		09.12.01	0.004	0.014	0.006	0.010	0.002	−0.008
		10.12.01	0.011	0.007	0.009	−0.004	−0.002	0.002
1004+130	LDQ	18.02.01	0.000	0.000		0.000		
		24.03.01	−0.003	0.001		0.004		
		29.03.00	0.002	0.005		0.003		
		30.03.00	0.021	0.028		0.007		
		16.03.99	0.077	0.089		0.012		
		27.02.99	0.081	0.099		0.018		
1128+310	CDQ	18.01.01	0.000	0.000	0.000	0.000	0.000	0.000
		09.03.02	0.135	0.136	0.130	0.001	−0.005	−0.006
		10.03.02	0.037	0.136	0.132	−0.001	−0.006	−0.004
1252+020	RQQ	09.03.00	0.000	0.000		0.000		
		03.04.00	0.006	0.002		−0.003		
		18.03.02	0.087	0.082		−0.005		
		26.04.01	0.177	0.183		0.006		
0134+329	LDQ	07.11.01	0.000	0.000	0.000	0.000	0.000	0.000
		08.11.01	0.002	−0.001	−0.001	−0.003	−0.004	0.000
		13.11.01	0.008	0.016	0.013	0.008	0.005	−0.003
1512+370	LDQ	21.04.02	0.000	0.000	0.000	0.000	0.000	0.000
		23.04.02	0.031	0.025	0.023	−0.005	−0.008	−0.002
		01.05.02	0.033	0.027	0.030	−0.006	−0.003	0.003
		27.03.02	0.054	0.048	0.047	−0.005	−0.007	−0.002
		23.03.02	0.085	0.082	0.082	−0.003	−0.003	0.001
0851+202	BL	31.12.99	0.000	0.000	0.000	0.000	0.000	0.000
		29.12.98		0.601	0.695			0.094
		28.03.00	0.936	0.928	0.906	−0.009	−0.031	−0.020
		17.02.01	1.631	1.628	1.624	−0.004	−0.007	−0.003
1101+319	RQQ	04.04.00		0.000	0.000			0.000
		22.04.01		0.041	0.042			0.000
		21.04.01		0.052	0.050			−0.003
		12.03.99		0.193	0.184			−0.009
1103−006	LDQ	06.04.00	0.000	0.000	0.000			
		17.03.99	0.018	0.018	−0.004			
		18.03.99	0.021	0.021	−0.001			
		14.04.01	0.316	0.314	−0.003			
		25.03.01	0.318	0.314	−0.005			
		22.03.02	0.329	0.324	−0.006			

Table 4. (*Continued*)

Object	Type	Date	Q-S1 (mag)	Q-S2 (mag)	Q-S3 (mag)	S1-S2 (mag)	S1-S3 (mag)	S2-S3 (mag)
1216−010	CDQ	15.03.02	0.000	0.000		0.000		
		11.03.02	0.087	0.085		−0.001		
		13.03.02	0.106	0.102		−0.003		
		16.03.02	0.140	0.135		−0.004		
0735+178	BL	26.12.98	0.000		0.000		0.000	
		30.12.99	0.457		0.465		0.008	
		24.12.01	0.720		0.715		−0.005	
		25.12.00	1.145		1.147		0.002	
0709+370	LDQ	20.01.01	0.000	0.000	0.000	0.000	0.000	0.000
		25.01.01	0.005	0.002	0.003	−0.003	−0.002	0.001
		21.01.01	0.004	0.005	0.006	0.001	0.002	0.000
		21.12.01	0.025	0.017	0.021	−0.008	−0.004	0.004
		20.12.01	0.040	0.029	0.033	−0.011	−0.008	0.004
0955+326	CDQ	19.02.99	0.000		0.000		0.000	
		03.03.00	0.044		0.057		0.013	
		05.03.00	0.047		0.060		0.013	
0219+428	BL	24.10.00	0.000		0.000		0.000	
		26.10.00	0.255		0.256		0.001	
		24.11.00	0.277		0.281		0.003	
		01.11.00	0.331		0.330		−0.001	
		13.11.99	0.449		0.449		0.000	
		01.12.00	0.622		0.631		0.010	
		14.11.98	0.691		0.684		−0.007	
0748+294	BL	13.01.99	0.000	0.000	0.000	0.000	0.000	0.000
		25.12.01	0.231	0.221	0.214	−0.010	−0.017	−0.007
		24.11.00	0.231	0.221	0.210	−0.009	−0.021	−0.012
		01.12.00	0.237	0.226	0.209	−0.010	−0.028	−0.017
		14.12.98	0.239	0.236	0.207	−0.002	−0.031	−0.029
		09.12.99	0.242	0.238	0.234	−0.004	−0.008	−0.004
0350−073	LDQ	14.11.01	0.000	0.000	0.000	0.000	0.000	0.000
		18.11.01	0.000	−0.001	−0.001	0.000	0.000	0.000
		15.11.01	0.000	0.005	0.006	0.002	0.003	0.002
1308+326	BL	26.04.00	0.000	0.000		0.000		
		03.05.00	0.016	0.009		−0.006		
		23.03.99	0.204	0.203		0.000		

LTOV nature of 11 quasars (6 CDQs and 5 BLs) are discussed by SSGW04, while the light curves for another 3 quasars (2 LDQs and 1 RQQ) are presented by SGSW04. Here we present the LTOV light curves of the remaining 12 objects (Figs. 7 and 8) of our sample and comment on those individual sources in increasing order of redshift.

LDQ 2349−014, $z = 0.174$: This QSO was monitored for three epochs which covered a time baseline of only five days. Over this time span the QSO was found to vary significantly. It faded by about 0.03 mag over four days between 13th October 2001 and 17th October 2001 and within the next 24 hours it brightened by about 0.05 mag (Fig. 8).

RQQ 0945+438, $z = 0.226$. This object was observed on three epochs and the time baseline extends over nearly three years. As neither of the comparison stars remained stable between our first epoch and the subsequent two epochs, we have considered

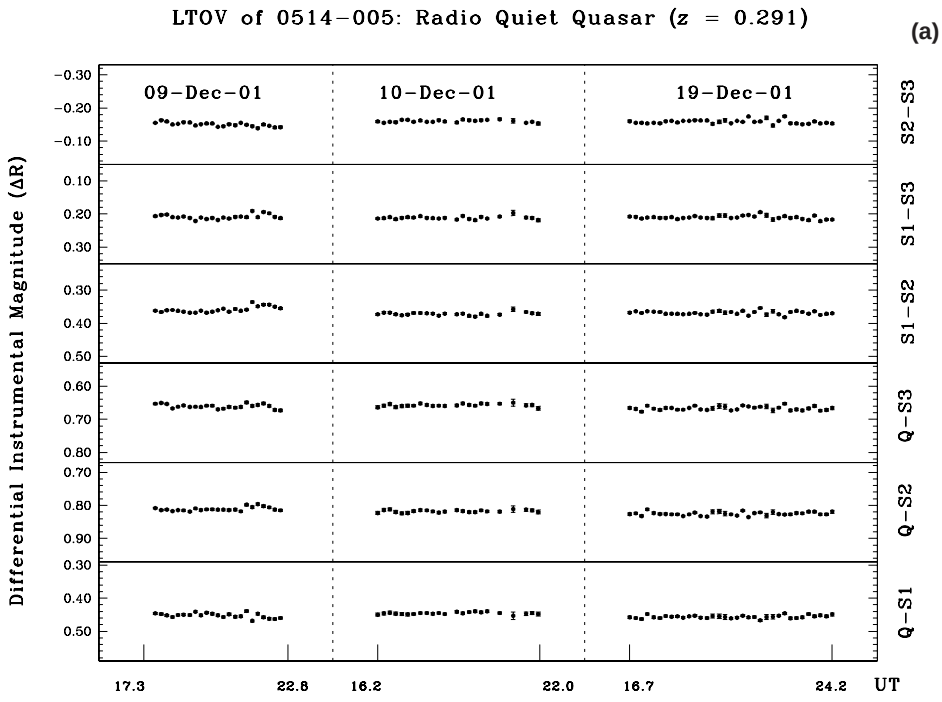

Figure 7. (*Continued*)

only the latter two epochs 26th February 2000 and 23rd January 2001 to examine the LTOV. The quasar dimmed by 0.07 mag within about a year between the two epochs (Fig. 7).

RQQ 0514−005, $z = 0.291$. Our three epochs of observations of this quasar covered a time baseline of only 11 days. The QSO did not show any change in brightness in about 24 hours between the first two epochs, but it faded by about 0.01 mag between 10th December 2001 and 19th December 2001 (Fig. 7).

RQQ 1252+020, $z = 0.345$: This QSO was monitored for five epochs; however, for LTOV only four epochs could be considered as the first epoch (22nd March 1999) lacks common comparison stars with the later four epochs. The total time baseline covered was about 2 years. The quasar remained at the same brightness level during the first two epochs of observations (9th March 2000 and 3rd April 2000). It brightened by about 0.18 mag when observed a year later on 26th April 2001. Observations on 18th March 2002 showed the object to have dimmed by about 0.10 mag compared to 26th April 2001 (Fig. 7).

LDQ 0134+329, $z = 0.367$: Three nights of observations were taken for this object, but they cover a time baseline of just six days. The object remained at the same brightness level during the first two days (7th and 8th November 2001), but dimmed by about 0.02 mag when observed again on 13th November 2001 (Fig. 8).

LDQ 1512+370, $z = 0.370$: This quasar was monitored on five epochs covering a time baseline of about 40 days. The object showed a gradual fading by about 0.09 mag between the first (23rd March 2002) and the third epochs (21st April 2002). It bright-

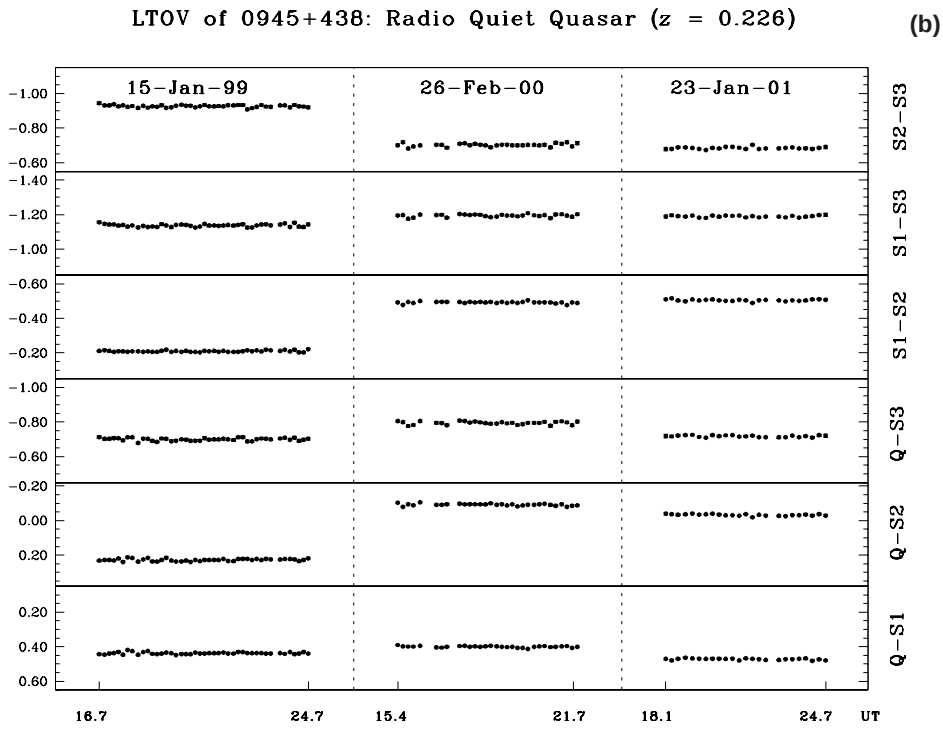

Figure 7. (*Continued*)

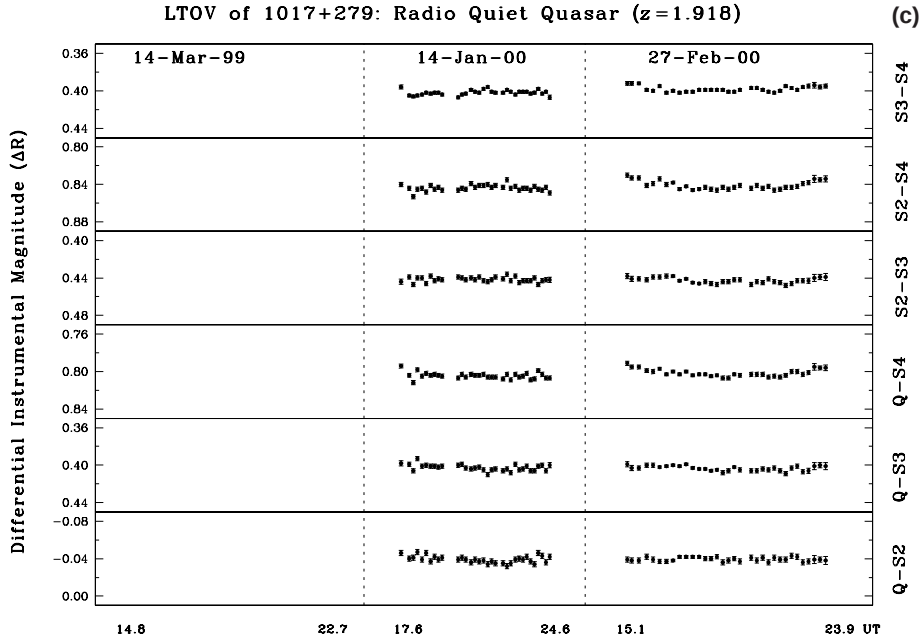

Figure 7. (*Continued*)

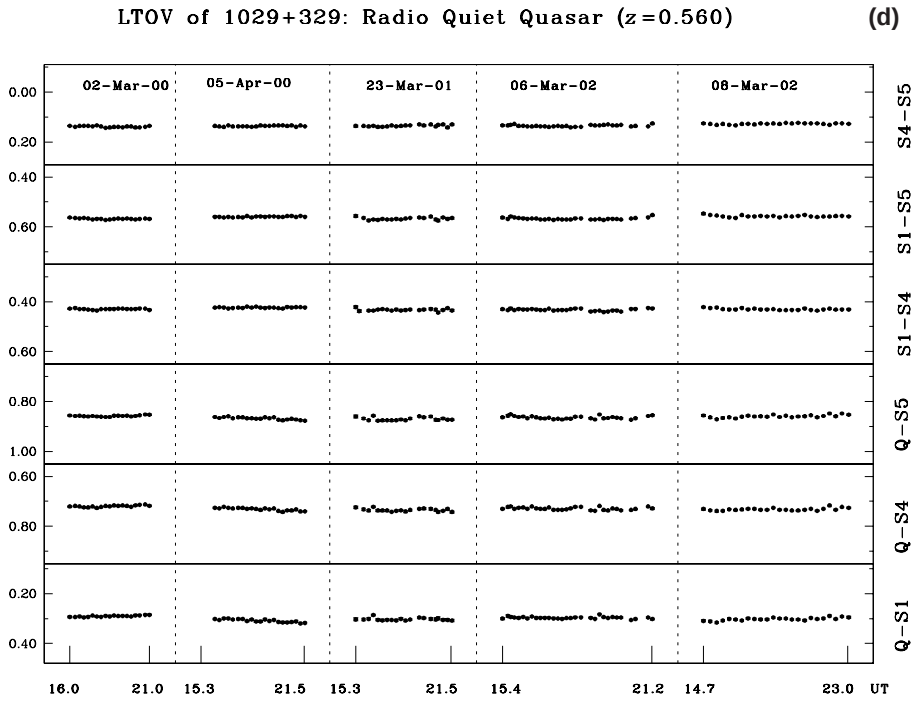

Figure 7. (*Continued*)

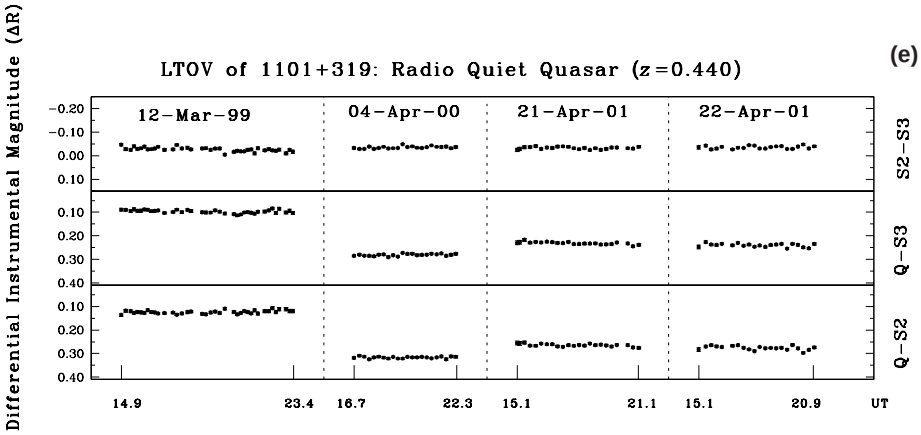

Figure 7. (*Continued*)

ened by about 0.03 mag when observed two days later on 23rd April 2002 and remained at the same brightness level during the last epoch of our observations (1st May 2002) (Fig. 8).

RQQ 1101+319, $z = 0.440$: Both brightening and fading were clearly present in our four epochs of observations which cover a time baseline of about two years. A fading

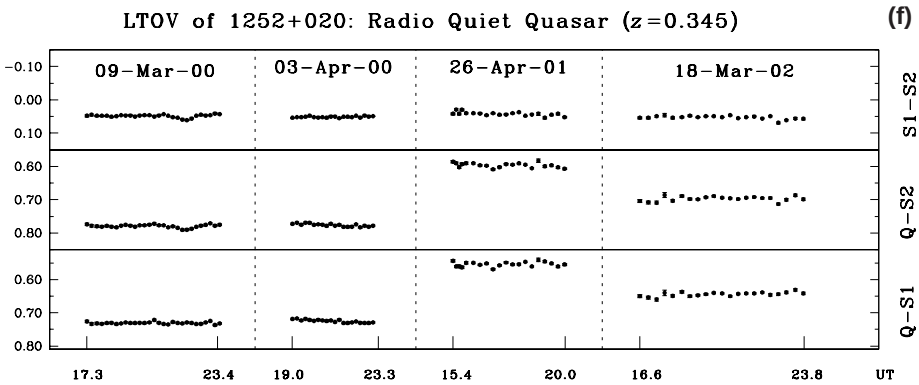

Figure 7(a–f). Long term variability of 6 radio-quiet quasars observed in this programme.

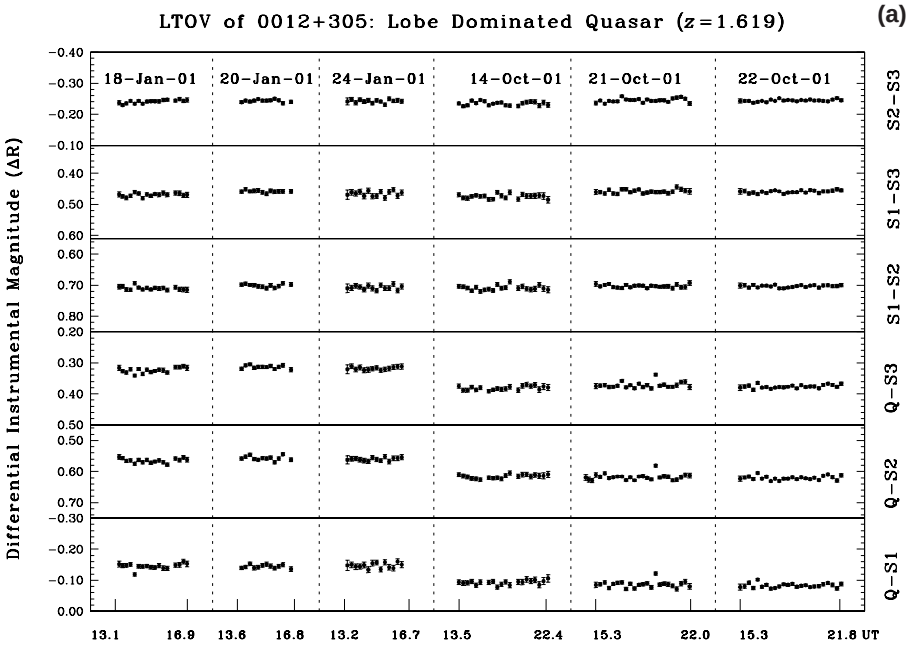

Figure 8. (*Continued*)

of about 0.19 mag was noticed in a year between the first two epochs of observations (12th March 1999 and 4th April 2000). When observed a year later (21st April 2001) a reversal in this trend was noticed whereby the quasar brightened by about 0.06 mag and thereafter remained fairly steady during the next 24 hours (Fig. 7).

LDQ 0709+37, $z = 0.487$: The LTOV of this QSO can be gleaned from the five epochs of observations done in the year 2001. It remained at the same brightness level during the first three epochs of observations during January 2001. However, it

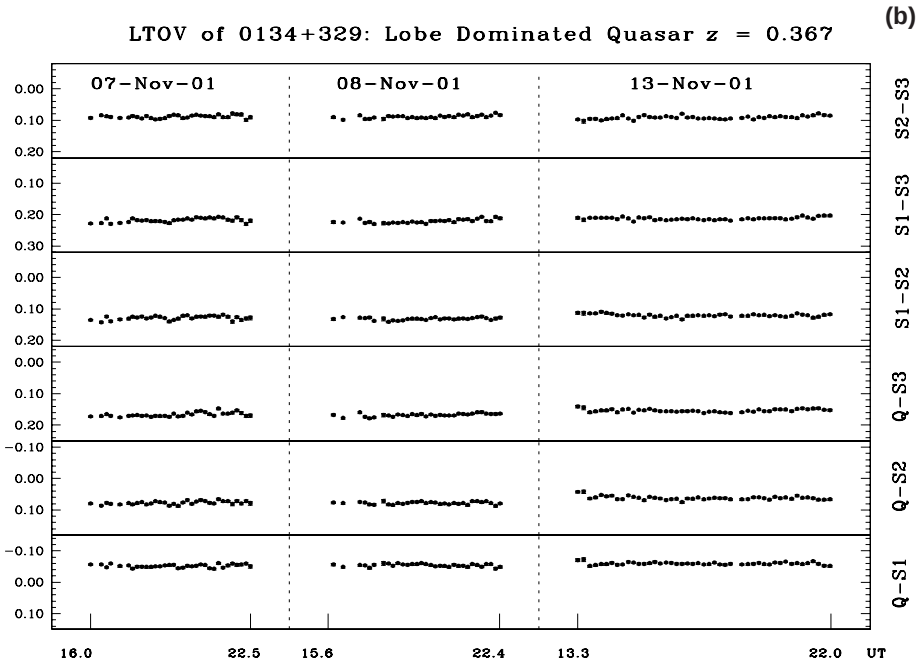

Figure 8. (*Continued*)

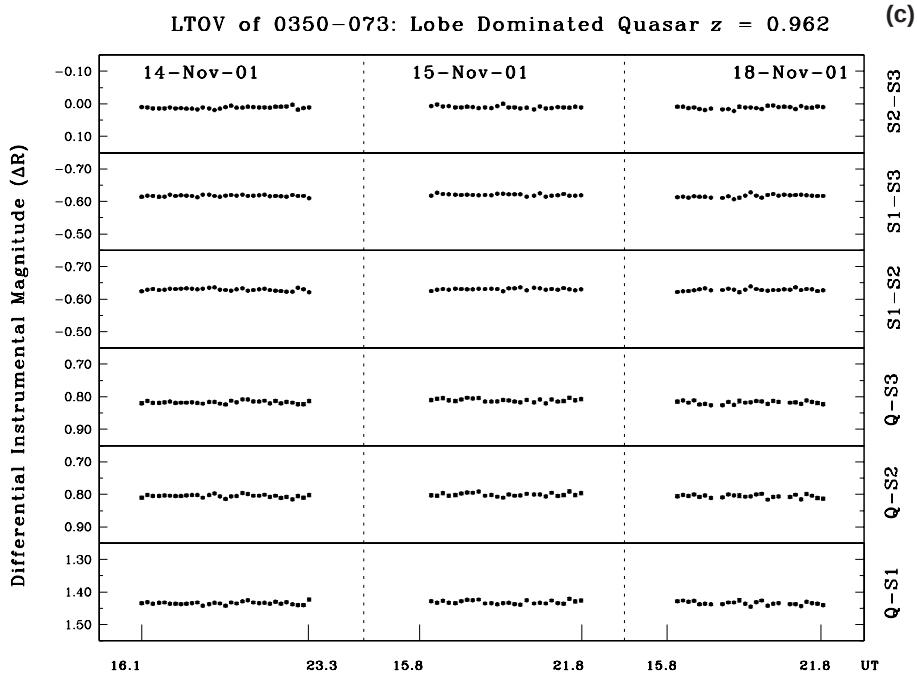

Figure 8. (*Continued*)

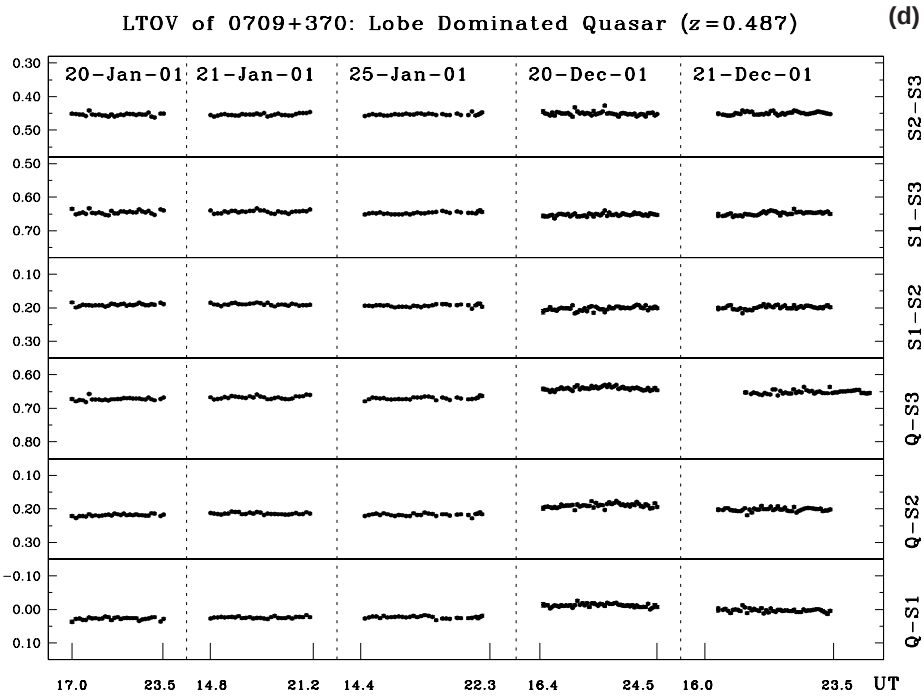

Figure 8. (*Continued*)

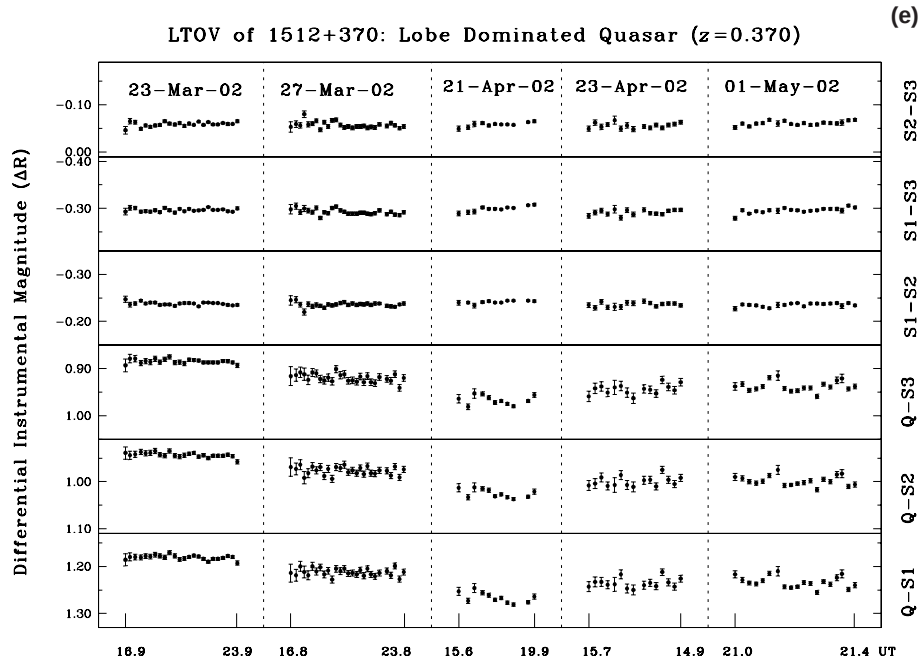

Figure 8. (*Continued*)

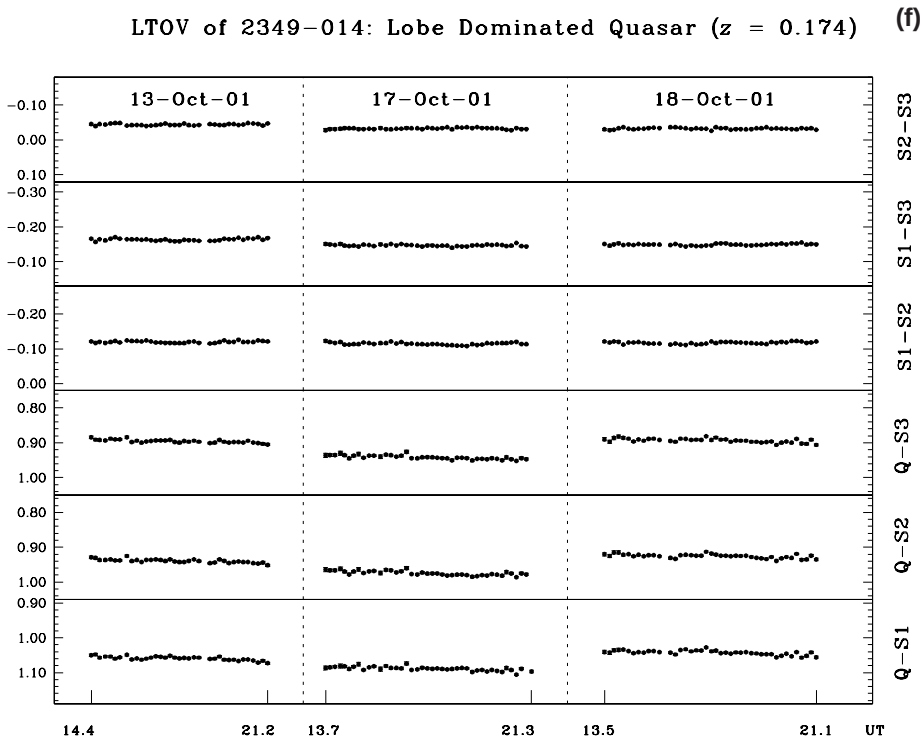

Figure 8(a–f). Long term variability of 6 lobe-dominated quasars observed in this programme.

brightened by about 0.03 mag when observed on 20th December 2001 and then faded by about 0.09 mag within the next 24 hours (between 20th and 21st December 2001; see Fig. 8).

RQQ 1029+329, $z = 0.560$: This QSO was monitored on six nights; however, for characterizing the LTOV only the later five epochs were considered due to the lack of common comparison stars in the first epoch of observation. The QSO remained at the same brightness level during our last five epochs of observations (between 2nd March 2000 and 8th March 2002) covering a two year baseline (Fig. 7).

LDQ 0350−073, $z = 0.962$: The quasar was found not to show any variability during our three epochs of observations within a week (during 14th to 18th November 2001) (Fig. 8).

LDQ 0012+305, $z = 1.619$. The quasar was found to be variable from our six epochs of observations encompassing about 10 months during 2001. It remained at the same brightness level during the first three epochs of observations and then faded by about 0.06 mag when observed nine months later on 14th October 2001. It then remained at the same brightness level for the next week during which it was monitored on three nights (Fig. 8).

RQQ 1017+279, $z = 1.918$. This quasar was monitored on three epochs. However, its LTOV could only be probed from the later two epochs, due to the lack of common comparison stars between them and the first epoch. The quasar remained at the same

flux level between the last two epochs (i.e., 14th January 2000 and 27th February 2000) separated by seven weeks (Fig. 7).

7. Do INOV and LTOV of blazars have a common origin?

A perception has gradually evolved that the most common cause of rapid optical variability of blazars is associated with disturbance occurring within their relativistic jets. For instance, Romero *et al.* (1999) have argued that while the LTOV arises due to large-scale relativistic shocks propagating through the jet, the INOV occurs due to the interception of these shocks by small scale magnetic irregularities in the jet. Similarly, Marscher *et al.* (1992) suggested that turbulence interacting with the shock could neatly explain the fast variations. To support or falsify these ideas, one needs to have a very large database of INOV monitoring observations at multiple epochs. Although such a compendium does not yet exist, our fairly extensive monitoring allows us to perform a check by searching for a correlation between the INOV amplitude and the level of optical brightness of the quasar.

If indeed both INOV and LTOV are phenomena related to relativistic jets then the best objects to look for the (presumably positive) correlation between them are blazars, for which at least the association of LTOV with the jet is rather secure (e.g., Hughes *et al.* 1992). To do this we have considered only the AGN for which we have LTOV data extending over at least two year baselines and for which INOV was clearly detected on at least two nights. For these 4 BL Lacs the values of INOV and LTOV for different nights are taken from Tables 2 and 4 respectively, and are plotted in Fig. 9. In no object, a clear correlation is seen between the INOV and LTOV amplitudes for these luminous AGNs whose optical emission is believed to be dominated by relativistic jets. In addition to the 4 objects plotted in Fig. 9, two additional BL Lacs, two RQQs and 1 CDQ also showed INOV on two or more occasions, but with total time spans less than two years; for these objects too, no correlations were found between INOV and LTOV. Thus, from an observational point of view, there is as yet no strong case for common origin of LTOV and INOV in the optical output of blazars.

7.1 *Do accretion disks contribute to INOV?*

The relation of INOV to the long term variability nature of quasars can be used to ascertain the contribution of any possible disk emission fluctuations to INOV (e.g., Mangalam & Wiita 1993; Wiita 1996; Xiong *et al.* 2000). Several Optically Violent Variables (OVV) including 3C 345 (Bregman *et al.* 1986; Smith *et al.* 1986), PKS $0420-014$, B2 $1156+295$ and 3C 454.3 (Smith *et al.* 1988) supply photometric and polarimetric evidence for substantial accretion disk contributions to their emission. But the general absence of a Big Blue Bump in BL Lac amounts to a lack of an accretion disk component that exists in most quasars (Sun & Malkan 1989). Still it has been claimed that in one of the best studied BL Lacs, $2155-304$, an accretion disk does seem to contribute to the spectrum (Wandel & Urry 1991), although, optical polarimetry implies that any disk contribution, if present, is fairly small (Smith & Sitko 1991).

If INOV is found to be inversely correlated to the brightness state of the object this may provide evidence for an accretion disk contribution to the observed INOV. This is because the disk component will be relatively more prominent when the object is in a quiescent state and jets are weaker. We again refer to Fig. 9 for a comparison of

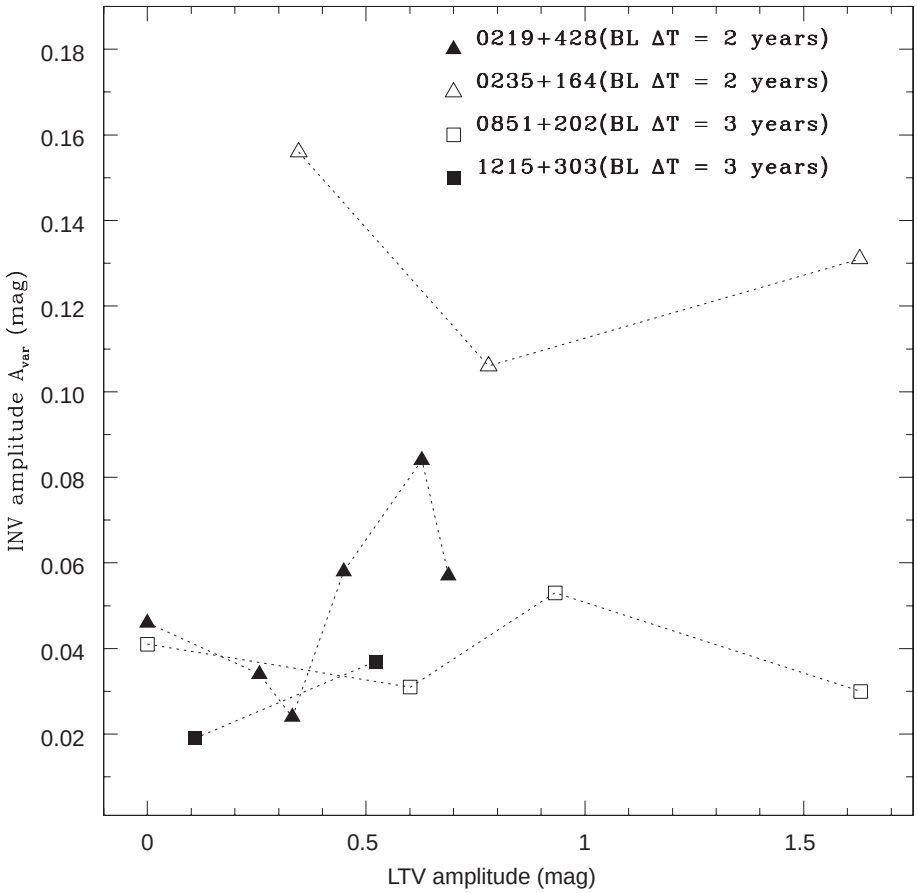

Figure 9. Comparison of INOV against LTOV.

INOV against LTOV for all the BL Lacs in our sample with significant LTOV time spans. No inverse correlation between INOV and LTOV is noticed, suggesting little contribution of an accretion disk to the observed INOV in any of these sources. Of course this dataset is so small that no firm conclusions in this regard can be drawn, and much larger studies are required. Some additional data in the literature (e.g., Carini *et al.* 1998) is also in accord with these results.

7.2 *INOV in the context of the starburst models of AGN*

In the starburst model (Terlevich *et al.* 1992; Terlevich & Melnik 1985) of AGNs, variability results from random superposition of events such as supernova explosions generating rapidly evolving compact supernova remnants (cSNRs) due to the interaction of their ejecta with the putative high density circumstellar environment. This model is supported by the striking similarity between the optical spectra of some AGNs and of cSNRs (Filippenko *et al.* 1989). The characteristics of an event (i.e., light curve, amplitude and time-scale) results from the combination of complicated processes (Terlevich

et al. 1992). Still, the lightcurves of AGNs of various absolute luminosities and redshifts can be predicted from the model and are found to be reasonably consistent with the observed dependence of the structure functions on luminosity and redshift (Fernandes, Aretxaga & Terlevich 1996; Cristiani *et al.* 1996). The lightcurves of cSNRs are still poorly known. While they seem to be consistent with the optical lightcurves of the low luminosity AGNs, NGC 4151 and NGC 5548 (Aretxaga & Terlevich 1994), as argued by Fernandes, Aretxaga & Terlevich (1997) and references therein, starburst models may be useful in explaining variability of modest amplitude in very weak AGN ($M_B \sim -20$ is the peak of a cSNR). As the energies involved in the intra-night fluctuations we have detected are at least an order of magnitude above the maxima expected from these SN models, it appears that they are not applicable to the variability events associated even with the non-blazar type luminous AGNs (Tables 2 and 4).

8. Conclusions

In this extensive optical monitoring programme, an effort has been made to understand the INOV characteristics of the four major classes of luminous AGNs, namely radio-quiet quasars, radio-lobe dominated quasars, radio-core dominated quasars and BL Lac objects. While the sample size, particularly for RQQs, is larger than previous studies, and our level of precision in obtaining INOV results is better than in most previous efforts, the sample size is still too small to provide absolutely firm conclusions. Bearing in mind that caveat, the major finding of this present study, which subsumes and refines those given in GSSW03, SGSW04, and SSGW04 are:

1. The first clear evidence of INOV in RQQs has been found from this observational programme (GSSW03). We have verified the radio-quiet nature of two members of this sample from VLA observations.
2. BL Lac objects are found to show a high DC of INOV (61%). In contrast, LDQs, CDQs and RQQs show smaller, comparable, INOV duty cycles ($\sim$ 20%). Our estimate of the DC of RQQs is much higher than 3% found by Romero *et al.* (1999); we attribute this to our better sensitivity, allowing us to claim detections that earlier observers could not see. Still, we find there is a marked difference between the INOV properties of blazars and radio-quiet quasars, in contrast to the conclusions reached by de Diego *et al.* (1998), namely that INOV occurs as frequently in RQQs as it does in all RLQs. This different conclusion of ours is probably due to both our higher sensitivity, and temporally much denser monitoring achieved in our program compared to that of de Diego *et al.* (1998).
3. The high DCs and amplitudes of variations shown by BL Lacs strongly suggests that relativistic beaming plays an important role in their observed INOV. Nonetheless, the much lower DC and amplitude of INOV, shown by LDQs and RQQs may still be understood within the framework of unified models, as the jets of these objects are believed to be modestly misaligned from our direction (see GSSW03; SSGW04). In those papers, we argued that LDQs and even RQQs could possess relativistic, optical synchrotron nuclear jets on micro-arcsecond scales. Their intrinsic optical variability might thus be similar to BL Lacs, as we showed that their observed milder INOV could be attributed to their (micro) jets being modestly misaligned from our direction (and so having lower Doppler factors, δ).

Thus, the observed difference in the micro-variability nature of LDQs and RQQs compared to BL Lacs could be accounted for in terms of their optically emitting nuclear jets undergoing different degrees of Doppler boosting in our direction. Observers located in suitably different directions may well find these same LDQs and RQQs to be large-amplitude rapid variables (GSSW03).

4. For blazars, no positive correlation is noticed between the INOV amplitude and the apparent optical brightness (Fig. 9). This suggests that the physical mechanisms for intra-night and long-term optical variability do not have a one-to-one relationship, and other factors are involved. Likewise, the absence of a clear negative correlation between the INOV and LTOV characteristics of the blazars in our sample points toward an inconspicuous contribution of the accretion disk to the observed INOV, though we stress that our sample size is very small and no firm conclusions can yet be drawn.
5. An apparent distinction is found for the first time between the INOV properties of the two classes of relativistically beamed radio-loud AGNs (RLQs), namely, BL Lacs and CDQs. The latter are found to exhibit a rather low INOV duty cycle, roughly that exhibited by RQQs and LDQs. Moreover BL Lacs show higher amplitude and DC of INOV. But in considering only the single CDQ which has high optical polarization $1216-010$, we found that it resembles BL Lacs, both in amplitude and DC of INOV. It thus appears that the mere presence of a prominent (and hence presumably Doppler boosted) radio core does not guarantee INOV; instead, it may well be that the more crucial factor is the optical polarization of the core emission. Such polarized emission is normally associated with shocks in a relativistic jet. This may suggest that the INOV is associated predominantly with highly polarized quasars (see SSGW04); however, it must be stressed that our sample of CDQs is too small to assign a strong level of confidence to this fascinating result.
6. Even though the percentage luminosity variations implied by the INOV for these luminous AGNs is small, the total power involved is still so enormous so as to render a starburst/supernova explanation untenable for these rapid events.

Additional monitoring of a variety of AGN types are necessary to verify the results we have presented here. While data on BL Lacs is reasonably good at this point (e.g. Carini *et al.* 1998 and references therein), more detailed studies of additional RQQs and both high- and low-polarized CDQs are absolutely necessary.

Acknowledgements

The help rendered by the technical staff at the 104 cm telescope of ARIES, Nainital is thankfully acknowledged. This research has made use of the NASA/IPAC Extragalactic Database (NED), which is operated by the Jet Propulsion Laboratory, California Institute of Technology, under contract with the National Aeronautics and Space Administration. The anonymous referee is thanked for comments which helped in improving the paper. CSS thanks NCRA for hospitality and use of its facilities and is also grateful for hospitality at GSU, where some revisions to this paper were carried out. PJW's efforts were partially supported by Research Program Enhancement funds to PEGA at GSU, and he is grateful for the continuing hospitality at Princeton University Observatory.

References

Angel J. R. P., Stockman H. S. 1980, *ARA&A*, **18**, 321.
Aretxaga I., Terlevich R. 1994, *MNRAS*, **269**, 462.
Bessel M. S. 1979, *PASP*, **91**, 589.
Berriman G., Schmidt G. D., West S. C., Stockman H. S. 1990, *ApJS*, **74**, 869.
Blandford R. J. 2000, *Trans. Roy. Soc. A*, **358**, 811.
Blandford R. J., Rees M. J. 1978, in Pittsburgh Conference on BL Lac Objects, (ed.) A. Wolfe (U. Pittsburgh) p. 328.
Blundell K. M., Beasley A. J. 1998, *MNRAS*, **299**, 165.
Blundell K. M., Rawlings S. 2001, *ApJL*, **562**, L5.
Boyle B. J., Shanks T., Croom S. M., Smith R. J., Miller L., *et al.* 2000, *MNRAS*, **317**, 1014.
Bregman J. N., Glassgold A.E., Huggins P. J., Kinney A. L. 1986, **301**, 708.
Carini M. T. 1990, Ph.D. thesis, Georgia State University, Atlanta, USA.
Carini M. T., Miller H. R., Noble J. C., Goodrich B. D. 1992, *AJ*, **104**, 15.
Carini M. T., Noble J. C., Miller H. R. 1998, *AJ*, **116**, 2667.
Carini, M., Noble, J., Amadi, O., Fendley, C., Simmons, De., Williams, S. 1999, *BAAS*, **31**, 1397.
Cellone S. A., Romero G. E., Combi J. A. 2000, *AJ*, **119**, 1534.
Cirasuolo M., Magliocchetti A., Celloti A., Danese L. 2003 (astro-ph/0301526).
Cristiani S., Trentini S., La Franca F., Aretxaga I., Andreani P., Vio R., Gemmo A. 1996, *A&A*, **306**, 395.
de Diego J. A., Dultzin-Hacyan D., Ramirez A., Benitez E. 1998, *ApJ*, **501**, 69.
Dunlop J. S., McLure R. J., Kukula M. J., Baum S. A., O'Dea C. P., Hughes D. H. 2003, *MNRAS*, **340**, 1095.
Edelson R. A., Turner T. J., Pounds K., Vaughan S., *et al.* 2002, *ApJ*, **568**, 610.
Elvis M., Wilkes B. J., McDowell J. C., Green R. F., Bechtold J., Willner S. P., Oey M. S., Polomski E., Curti R. 1994, *ApJS*, **95**, 1.
Fabian A. C., Rees M. J. 1979, in X-ray Astronomy (eds) W. A. Barty and L. E. Peterson (Oxford: Pergamon Press) p. 381.
Falcke H., Patnaik A. R., Sherwood W. 1996, *ApJ*, **473**, L13.
Fernandes C. R., Terlevich R., Aretxaga I. 1997, *MNRAS*, **289**, 318.
Fernandes C. R., Aretxaga I, Terlevich R. 1996, *MNRAS*, **282**, 1191.
Filippenko A. V. 1989, *AJ*, 97, 726.
Frank J., King A. R., Raine D. J. 1986, Accretion Power in Astrophysics (Cambridge: Cambridge University Press).
Garcia A., Sodre L., Jablonski F. J., Terlevich R. J. 1999, *MNRAS*, **309**, 803.
Goldschmidt, P., Kukula, M. J., Miller, L., Dunlop, J. S. 1999, *ApJ*, **511**, 612.
Gopal-Krishna, Sagar R., Wiita P. J. 1995, *MNRAS*, **274**, 701.
Gopal-Krishna, Gupta A. C., Sagar R., Wiita P. J., Chaubey U. S., Stalin C. S. 2000, *MNRAS*, **314**, 888.
Gopal-Krishna, Stalin C. S., Sagar R., Wiita P. J. 2003, *ApJ*, **586**, L25 (GSSW03).
Ho L. C. 2002, *ApJ*, **564**, 120.
Heidt J., Wagner S. J. 1996, *A&A*, **305**, 42.
Henden A. A., Kaitchuck R. H. 1982, Astronomical Photometry, p. 52 (Van Nostrand Reinhold, New York).
Howell S. B. 1989, *PASP*, **101**, 616.
Hughes P. A., Aller A. D., Aller M. F. 1992, *ApJ*, **396**, 469.
Hutsemekers D., Lamy H. 2001, *A&A*, **367**, 381.
Ivezic Z., *et al.* 2002, *AJ*, **124**, 2364.
Jang M., Miller H. R. 1995, *ApJ*, **452**, 582.
Jang M., Miller H. R. 1997, *AJ*, **114**, 565.
Kellermann K. I., Sramek R., Schmidt M., Shaffer D. B., Green R. 1989, *AJ*, **98**, 1195.
Kellermann K. I., Sramek R. A., Schmidt M., Green R. F., Shaffer D. B. 1994, *AJ*, **108**, 1163.
Kellermann K. I., *et al.* 2004, *ApJ*, in press (astro-ph/0403320).
Kukula M. J., Dunlop J. S., Hughes D. H., Rawlings S. 1998, *MNRAS*, **297**, 366.
Kundt W. 2002, *New Astronomy Reviews*, **46**, 257.
Mangalam A. V., Wiita P. J. 1993, *ApJ*, **406**, 420.
Marscher A. P., Gear W. K. 1985, *ApJ*, **298**, 114.

Marscher A. P., Gear W. K., Travis J. P. 1992, in *Variability of Blazars*, (eds.) E. Valtaoja, M. Valtonen (Cambridge: Cambridge Univ. Press) p. 85.
Marscher A., Scott J. S. 1980, *PASP*, **92**, 127.
McLure R. J., Dunlop J. 2001 in *QSO hosts and their environments*, (eds.) I. Marquez, *et al.* (Dordrecht: Kluwer) p. 27.
Meier D. L. 2002, *New Astronomy Reviews*, **46**, 247.
Miller P., Rawlings S., Saunders R. 1993, *MNRAS*, **263**, 425.
Miller H. R., Carini M. T., Goodrich B. D. 1989, *Nature*, **337**, 627.
Monet, D. G., *et al.* 2003, *AJ*, **125**, 984.
Noble J. C. 1995, *Ph.D. thesis, Georgia State University, Atlanta*, USA.
Paczyński B., Wiita P. J. 1980, *A&A*, **88**, 23.
Papadopoulos P. P., Seaquist E. R., Wrobel J. M., Binette L. 1995, *ApJ*, **446**, 150.
Quataert, E., Narayan, R. 1999, *ApJ*, **516**, 399.
Rabbette M., McBreen B., Smith N., Steel S. 1998, *A&AS*, **129**, 445.
Romero C. E., Cellone S. A., Combi J. A. 1999, *A&AS*, **135**, 477.
Sagar R., 1999, *Current Science*, **77**, 643.
Sagar R., Stalin, C. S., Gopal-Krishna, Wiita P. J. 2004, *MNRAS*, **348**, 176 (SSGW04).
Schmidt M., Green R. F. 1983, *ApJ*, **269**, 352.
Simonetti J. H., Cordes J. M., Heeschen D. S. 1985, *ApJ*, **296**, 46.
Smith P. S., Sikto M. L. 1991, *ApJ*, **383**, 580.
Smith P. S., Balonek T. J., Heckert P. A., Elston R. 1986, *ApJ*, **305**, 484.
Smith A. G., Leacock R. J., Webb J. R. 1988, in *Variability in Active Galactic Nuclei*, (eds.) H.R. Miller, P.J. Wiita (Berlin: Springer) p. 158.
Stalin C. S., Gopal-Krishna, Sagar R., Wiita P. J. 2004, *MNRAS*, **350**, 175 (SGSW04).
Stocke T. J., Morris S. L., Weymann R. J., Foltz C. B. 1992, *ApJ*, **396**, 487.
Sun W. H., Malkan M. A. 1989, *ApJ*, **346**, 68.
Terlevich R., Melnick J. 1985, *MNRAS*, **213**, 84.
Terlevich R., Tenorio-Tagle G., Franco J., Melnick J. 1992, *MNRAS*, **255**, 713.
Veron-Cetty M. P., Veron P. 1998, *ESO Scientific Report* No. 18.
Wandel A., Urry C. M. 1991, *ApJ*, **367**, 78.
White, R. L., *et al.* 2000, *ApJS*, **126**, 133.
Wiita P. J. 1996, in *Blazar Continuum Variability*, (eds.) H.R. Miller, J.R. Webb, J.C. Noble, *Astr. Soc. Pacific Conf. Ser.* 110, (ASP, San Francisco) p. 42.
Wills B. J. 1996, in *Jets from Stars and Galactic Nuclei, Lecture Notes in Physics*, Vol. **471**, (ed) W. Kundt, (Berlin: Springer) p. 213.
Wills B. J., Wills D., Breger M., Antonucci R. R. J., Barvainis R. 1992, *ApJ*, **398**, 454.
Wilson A. S., Colbert E. J. M. 1995, *ApJ*, **438**, 62.
Wisotzki L. 2000, *A&A*, **353**, 853.
Woo J. M., Urry C. M. 2002, *ApJ*, **581**, L5.
Worrall D. M. 1986, *ApJ*, **303**, 589.
Xiong, Y., Wiita, P. J., Bao, G. 2000, *PASJ*, **52**, 1097.
Zhang L. Z., Fan J. H., Cheng K. S. 2002, *PASJ*, **54**, 159.